

Next-to-Leading Order NMSSM Decays with CP-odd Higgs Bosons and Stops

J. Baglio^{1,*}, C.O. Krauss^{2,†}, M. Mühlleitner^{2,‡}, K. Walz^{2,§}

¹*Institute for Theoretical Physics, Tübingen University,
Auf der Morgenstelle 14, 72076 Tübingen, Germany*

²*Institute for Theoretical Physics, Karlsruhe Institute of Technology,
Wolfgang-Gaede-Str. 1, 76131 Karlsruhe, Germany*

Abstract

We compute the full next-to-leading order supersymmetric (SUSY) electroweak (EW) and SUSY-QCD corrections to the decays of CP-odd NMSSM Higgs bosons into stop pairs. In our numerical analysis we also present the decay of the heavier stop into the lighter stop and an NMSSM CP-odd Higgs boson. Both the EW and the SUSY-QCD corrections are found to be significant and have to be taken into account for a proper prediction of the decay widths.

*E-mail: julien.baglio@kit.edu

†E-mail: carla.olivia.k@googlemail.com

‡E-mail: margarete.muehlleitner@kit.edu

§E-mail: kathrin.walz@kit.edu

1 Introduction

The announcement of the discovery of a new boson by the LHC experiments ATLAS [1] and CMS [2] has marked a milestone for particle physics. While the properties of this particle are consistent with the SM predictions, the uncertainties in the experimental data still leave enough room for interpretations in extensions beyond the SM. Among these, supersymmetric (SUSY) models [3] certainly belong to the best motivated and most intensely studied ones. In particular the Next-to-Minimal Supersymmetric Extension (NMSSM) [4] provides with the introduction of an additional complex superfield \hat{S} a dynamical solution to the μ problem [5] when the singlet field acquires a non-vanishing vacuum expectation value. Because of new contributions to the quartic coupling λ , with which \hat{S} couples to the Higgs doublet superfields \hat{H}_u and \hat{H}_d , the tree-level mass value of the lighter MSSM-like Higgs boson is enhanced. In consequence less important radiative corrections are required to shift the mass value to the measured value of 125 GeV and therefore smaller stop masses and/or mixing are necessary, so that the fine-tuning is reduced [6, 7].

After electroweak symmetry breaking (EWSB) the Higgs sector of the NMSSM consists of seven physical Higgs bosons. In the CP-conserving case, which we assume to be valid here, these are three neutral CP-even, two neutral CP-odd and two charged Higgs bosons. The discovery of all Higgs particles is challenging though not impossible at the high-energy option of the LHC. In [8] we investigated the discovery prospects for the NMSSM Higgs bosons during the 13 TeV run of the LHC and gave benchmark scenarios that feature Higgs-to-Higgs decays.¹ If kinematically allowed also decays into supersymmetric particles can become important, as is well known for the Minimal Supersymmetric Extension of the SM (MSSM) [37, 38]. The one-loop SUSY-QCD corrections to the decays into stops and sbottoms of the MSSM Higgs bosons have been calculated in [39–41] and can change the decay widths by more than 50%, especially near the threshold. The SUSY-QCD corrections have been reanalyzed in [42]. The full electroweak (EW) one-loop corrections to the pseudoscalar decays into squarks have been provided in [43] and have turned out to be significant. Equally, the decays of heavy squarks into lighter ones and a Higgs boson can dominate in a wide range of the MSSM parameter space due to the large Yukawa couplings and stop and sbottom mixing [44]. The SUSY-QCD corrections at next-to-leading order (NLO) are of the order of a few ten percent [45] and mostly negative. The one-loop EW corrections to the decays with a pseudoscalar in the final state are significant [43]. The full one-loop corrections for the complex MSSM have been discussed in [46].

The proper interpretation of the experimental data and, once SUSY has been discovered, the aim to pin down the underlying model and distinguish *e.g.* the NMSSM from the MSSM, require precise predictions both for the parameters of the model and for the observables like *e.g.* NMSSM Higgs boson production and decay rates [47]. The higher order corrections to the CP-conserving NMSSM Higgs boson masses and self-couplings have been given in [48–58] and [16], respectively. Additionally, there are several codes available for the evaluation of the NMSSM mass spectrum from a user-defined input at a user-defined scale, like `NMSSMTools` [59–61] which can be interfaced with `SOFTSUSY` [62, 63], the interface of `SARAH` [57, 64–67] with `SPheno` [68, 69], and finally `SARAH` which has been interfaced with the recently published package `FlexibleSUSY` [70, 71]. Recently, `NMSSMTools` has been extended to include also the CP-violating NMSSM [72]. In our Fortran package `NMSSMCALC` [73] we have included in the CP-conserving and CP-violating NMSSM the full one-loop and the order $\mathcal{O}(\alpha_t \alpha_s)$ corrections to the NMSSM Higgs boson masses [56, 74, 75] and

¹For other recent studies on NMSSM Higgs boson phenomenology, see Refs. [7, 9–36].

the state-of-the-art higher order corrections to the decays. These include in the CP-conserving case Higgs decays into stops and sbottoms the SUSY-QCD corrections of [42] which have been adapted from the MSSM to the NMSSM case. Very recently, neutral Higgs production through gluon fusion and bottom-quark annihilation including higher order corrections has been discussed in [76].

With this work we take another step in improving the predictions for the NMSSM Higgs sector. We provide both the NLO SUSY-QCD and the full one-loop EW corrections to the decays of a pseudoscalar NMSSM Higgs boson into stops as well as to the decays of the heavier stop into the lighter one and a pseudoscalar.

The paper is organized as follows. In section 2 we introduce the NMSSM Higgs sector and set our notation. The tree-level decay of a pseudoscalar Higgs into stops is discussed in section 3, before we present in section 4 the order $\mathcal{O}(\alpha_s)$ SUSY-QCD corrections and in section 5 the one-loop EW corrections. The numerical analysis, including the discussion of heavier stop decays into a pseudoscalar and lighter stop final state, is performed in section 6. We conclude in section 7.

2 The NMSSM Higgs Sector

The NMSSM Higgs potential is obtained from the NMSSM superpotential, which we assume to be scale invariant, the soft SUSY breaking terms and the D -term contributions, which are the same as in the MSSM. In terms of the superfields \hat{H}_u and \hat{H}_d , coupling to the up- and down-type quarks, respectively, and the singlet superfield \hat{S} the superpotential reads

$$W_{NMSSM} = W_{MSSM} - \epsilon_{ij} \lambda \hat{S} \hat{H}_d^i \hat{H}_u^j + \frac{1}{3} \kappa \hat{S}^3, \quad (2.1)$$

where $i, j = 1, 2$ are the $SU(2)_L$ indices and we have introduced the totally antisymmetric tensor ϵ_{ij} with $\epsilon_{12} = 1$. Working in the CP-invariant NMSSM, the dimensionless parameters λ and κ are chosen to be real. The MSSM superpotential W_{MSSM} is given by

$$W_{MSSM} = \epsilon_{ij} [y_e \hat{H}_d^i \hat{L}^j \hat{E}^c + y_d \hat{H}_d^i \hat{Q}^j \hat{D}^c - y_u \hat{H}_u^i \hat{Q}^j \hat{U}^c], \quad (2.2)$$

with the quark and lepton superfields and their charge conjugates, indicated by the superscript c , denoted by $\hat{Q}, \hat{U}^c, \hat{D}^c, \hat{L}$ and \hat{E}^c . The color and generation indices have been suppressed in Eq. (2.2). We neglect generation mixing of the quarks, so that the phases of the Yukawa couplings y_d , y_u and y_e , which in general are complex, can be reabsorbed by a redefinition of the quark fields. The soft SUSY breaking NMSSM Lagrangian involving the Higgs doublet and singlet component fields H_u , H_d and S reads

$$\mathcal{L}_{soft} = \mathcal{L}_{soft, MSSM} - m_S^2 |S|^2 + (\epsilon_{ij} \lambda A_\lambda S H_d^i H_u^j - \frac{1}{3} \kappa A_\kappa S^3 + h.c.), \quad (2.3)$$

with the soft SUSY breaking MSSM Lagrangian

$$\begin{aligned} \mathcal{L}_{soft, MSSM} = & -m_{H_d}^2 H_d^\dagger H_d - m_{H_u}^2 H_u^\dagger H_u - m_{\tilde{Q}}^2 \tilde{Q}^\dagger \tilde{Q} - m_{\tilde{L}}^2 \tilde{L}^\dagger \tilde{L} - m_{\tilde{U}_R}^2 \tilde{u}_R^* \tilde{u}_R - m_{\tilde{D}_R}^2 \tilde{d}_R^* \tilde{d}_R \\ & - m_{\tilde{E}_R}^2 \tilde{e}_R^* \tilde{e}_R - (\epsilon_{ij} [y_e A_E H_d^i \tilde{L}^j \tilde{e}_R^* + y_d A_D H_d^i \tilde{Q}^j \tilde{d}_R^* - y_u A_U H_u^i \tilde{Q}^j \tilde{u}_R^*] + h.c.) \\ & - \frac{1}{2} (M_1 \tilde{B} \tilde{B} + M_2 \tilde{W}_k \tilde{W}_k + M_3 \tilde{G} \tilde{G} + h.c.). \end{aligned} \quad (2.4)$$

The gaugino fields are denoted by \tilde{B} , \tilde{W}_k ($k = 1, 2, 3$) and \tilde{G} , and the left-handed squarks and sleptons are arranged in doublets denoted by $\tilde{Q} = (\tilde{u}_L, \tilde{d}_L)^T$, $\tilde{L} = (\tilde{\nu}_L, \tilde{e}_L)^T$ while the right-handed fields are denoted by \tilde{u}_R , \tilde{d}_R and \tilde{e}_R . The soft SUSY breaking mass parameters $m_{X(R)}^2$ of the scalar fields $X = S, H_d, H_u, \tilde{Q}, \tilde{U}, \tilde{D}, \tilde{L}, \tilde{E}$ are real, while the gaugino mass parameters M_1, M_2 and M_3 and the soft SUSY breaking trilinear couplings A_Y ($Y = \lambda, \kappa, U, D, E$) are in general complex. In the CP-conserving case assumed here, they are, however, real. Again, the respective quark and lepton superfields are understood to refer to all three fermion generations. Note that we have set soft SUSY breaking terms linear and quadratic in the singlet field S to zero.

After expanding the Higgs fields about their vacuum expectation values (VEVs) v_u , v_d and v_s , chosen to be real and positive,

$$H_d = \begin{pmatrix} (v_d + h_d + ia_d)/\sqrt{2} \\ h_d^- \end{pmatrix}, \quad H_u = \begin{pmatrix} h_u^+ \\ (v_u + h_u + ia_u)/\sqrt{2} \end{pmatrix}, \quad S = \frac{v_s + h_s + ia_s}{\sqrt{2}}, \quad (2.5)$$

the Higgs mass matrices for the three scalar, two pseudoscalar and the charged Higgs bosons can be derived from the tree-level scalar potential. The mass matrix decomposes into two mass matrices for the CP-even and the CP-odd Higgs fields. The squared 3×3 mass matrix M_S^2 for the CP-even Higgs fields can be diagonalized through a rotation matrix \mathcal{R}^S which yields the CP-even mass eigenstates H_i ($i = 1, 2, 3$) as

$$(H_1, H_2, H_3)^T = \mathcal{R}^S(h_d, h_u, h_s)^T. \quad (2.6)$$

The H_i are ordered by ascending mass, $M_{H_1} \leq M_{H_2} \leq M_{H_3}$. In order to obtain the CP-odd mass eigenstates A_1, A_2 and the massless Goldstone boson G first a rotation \mathcal{R}^G to separate G is applied, and then a rotation \mathcal{R}^P to obtain the mass eigenstates

$$(A_1, A_2, G)^T = \mathcal{R}^P(a, a_s, G)^T = \mathcal{R}^P \mathcal{R}^G(a_d, a_u, a_s)^T, \quad (2.7)$$

which are ordered such that $M_{A_1} \leq M_{A_2}$.

The minimisation of the Higgs potential V requires the terms linear in the Higgs fields to vanish in the vacuum. The corresponding coefficients, which are called tadpoles, therefore have to be zero. The tadpole conditions for the CP-even fields can be exploited to replace $m_{H_u}^2, m_{H_d}^2$ and m_S^2 by the tadpole parameters t_{h_d}, t_{h_u} and t_{h_s} . Replacing the $SU(2)_L$ and $U(1)_Y$ gauge couplings g and g' and the VEVs v_u and v_d by the electric charge e , the gauge boson masses M_W, M_Z and by $\tan \beta$, the tree-level NMSSM Higgs sector can then be parameterized by the twelve parameters

$$t_{h_u}, t_{h_d}, t_{h_s}, e, M_W^2, M_Z^2, \lambda, \kappa, A_\lambda, A_\kappa, \tan \beta = \langle H_u^0 \rangle / \langle H_d^0 \rangle \quad \text{and} \quad \mu_{\text{eff}} = \lambda \langle S \rangle. \quad (2.8)$$

The VEVs of the neutral components of the Higgs fields are denoted by the brackets around the corresponding fields. The sign conventions for λ and $\tan \beta$ are chosen such that they are positive. The $\kappa, A_\lambda, A_\kappa$ and μ_{eff} on the other hand can have both signs. Note also, that the parameter A_λ can be traded for the charged Higgs boson mass M_{H^\pm} , which we will do in the following. From now on we will drop the subscript 'eff'. Note that the inclusion of higher order corrections requires also the soft SUSY breaking mass terms for the scalars and the gauginos as well as the trilinear soft SUSY breaking couplings.

3 The Tree-level Decay Width

We start by discussing the tree-level decay width of a pseudoscalar Higgs boson A_i ($i = 1, 2$) into a pair of stops. The stop mass matrix in the interaction basis $(\tilde{t}_L, \tilde{t}_R)$ reads

$$\mathcal{M}_{\tilde{t}}^2 = \begin{pmatrix} m_{LL}^2 & m_{LR}^2 \\ m_{RL}^2 & m_{RR}^2 \end{pmatrix}, \quad (3.9)$$

with

$$m_{LL}^2 = m_{\tilde{Q}}^2 + m_t^2 + M_Z^2 \cos 2\beta \left(\frac{1}{2} - \frac{2}{3} \sin^2 \theta_W \right) \quad (3.10)$$

$$m_{RR}^2 = m_{\tilde{t}_R}^2 + m_t^2 + \frac{2}{3} M_Z^2 \cos 2\beta \sin^2 \theta_W \quad (3.11)$$

$$m_{LR}^2 = m_{RL}^2 = m_t(A_t - \mu \cot \beta), \quad (3.12)$$

in terms of the soft SUSY breaking mass parameters $m_{\tilde{Q}}$ and $m_{\tilde{t}_R}$, the soft SUSY breaking trilinear coupling A_t , the higgsino mixing parameter μ , the top and the Z boson masses m_t and M_Z , the mixing angle β and the Weinberg angle θ_W . The μ parameter is generated dynamically in the NMSSM and given by

$$\mu = \frac{\lambda v_s}{\sqrt{2}}. \quad (3.13)$$

The stop mass matrix is diagonalized by

$$\mathcal{R}^{\tilde{t}} = \begin{pmatrix} \cos \theta_{\tilde{t}} & \sin \theta_{\tilde{t}} \\ -\sin \theta_{\tilde{t}} & \cos \theta_{\tilde{t}} \end{pmatrix} \quad (3.14)$$

yielding the stop mass eigenstates \tilde{t}_i ($i = 1, 2$) as

$$\tilde{t}_i = \mathcal{R}_{is}^{\tilde{t}} \tilde{t}_s, \quad (3.15)$$

where $s = L, R$ and for the squark masses we have $m_{\tilde{t}_1} < m_{\tilde{t}_2}$ by convention. The mixing angle $\theta_{\tilde{t}}$ and the squark masses are given by

$$\tan \theta_{\tilde{t}} = \frac{2m_{LR}^2}{m_{LL}^2 - m_{RR}^2 - \sqrt{(m_{LL}^2 - m_{RR}^2)^2 + 4m_{LR}^4}} \quad (3.16)$$

and

$$m_{\tilde{t}_{1,2}}^2 = \frac{1}{2} \left[m_{LL}^2 + m_{RR}^2 \mp \sqrt{(m_{LL}^2 - m_{RR}^2)^2 + 4m_{LR}^4} \right]. \quad (3.17)$$

In case of the pseudoscalar only the coupling to two different stop mass eigenstates is non-vanishing. For the tree-level decay width Γ^{LO} we have

$$\Gamma^{\text{LO}}(A_i \rightarrow \tilde{t}_1 \tilde{t}_2) = \frac{3\lambda^{1/2}(M_{A_i}^2, m_{\tilde{t}_1}^2, m_{\tilde{t}_2}^2)}{8\pi M_{A_i}^3} \left| \sum_{j=1}^2 \mathbf{Z}_{ij} G_{A_j}^{12} \right|^2, \quad (3.18)$$

where $\lambda(x, y, z) = (x - y - z)^2 - 4yz$ is the two-body phase space function and the coupling $G_{A_j}^{12}$ ($j = 1, 2$) of the pseudoscalar A_j to the stops reads

$$G_{A_j}^{12} = \frac{gm_t}{2M_W} \left[\left(\frac{A_t}{\tan \beta} + \mu \right) \mathcal{R}_{j1}^P + \frac{\lambda v}{\sqrt{2} \tan \beta} \mathcal{R}_{j2}^P \right] \quad (3.19)$$

where v is the VEV given by $v^2 = v_u^2 + v_d^2$ and \mathcal{R}_{jk}^P are the elements of the rotation matrix defined in Eq. (2.7). In particular, they are the tree-level mixing matrix elements. In the kinematics of the decay, however, *i.e.* for the external Higgs field, we use the two-loop corrected Higgs boson masses at order $\mathcal{O}(\alpha_t \alpha_s)$, which include the full EW corrections at one-loop order. The renormalization of the Higgs fields and the computation of the mass corrections have been described in Refs. [56, 74, 75]. We follow the conventions of these papers, to which we refer the reader for more details. In order to ensure the on-shell properties of the external Higgs field, which in the calculation of the Higgs mass corrections has been renormalized in the mixed on-shell- $\overline{\text{DR}}$ scheme, the finite wave function renormalization factors \mathbf{Z} [77] have to be taken into account. The application of the factor \mathbf{Z} to the tree-level matrix \mathcal{R}^P (in $G_{A_j}^{12}$) leads to the rotation matrix $\mathcal{R}^{P,l}$ which, modulo the Goldstone boson G , rotates the interaction eigenstates a and a_s to the loop corrected mass eigenstates A_1 and A_2 , *cf.* [56],

$$\mathcal{R}_{il}^{P,l} = \mathbf{Z}_{ij} \mathcal{R}_{jl}^P, \quad i, j = A_1, A_2, G, \quad l = a, a_s, G. \quad (3.20)$$

These and the loop-corrected masses are taken from the Fortran code `NMSSMCALC` [73], in which we choose the on-shell (OS) renormalization for the top/stop sector in order to be in accordance with the renormalization scheme chosen later on both in the SUSY-QCD corrections and in the electroweak corrections.

In Eq. (3.18) we have summed over both possible final states $\tilde{t}_1 \tilde{t}_2^*$ and $\tilde{t}_1^* \tilde{t}_2$. In the MSSM, *i.e.* leaving out the singlet contribution $\propto \lambda$ in the coupling $G_{A_i}^{12}$, the decay width is proportional to $m_t^2(\mu + A_t/\tan \beta)^2/M_{A_i}$. For small values of $\tan \beta$ and not too heavy pseudoscalars, the decay into stops can compete with and even dominate over the decays into top quarks and into charginos and neutralinos. In the NMSSM, this statement has to be taken with caution, however, as the singlet component in the coupling $G_{A_i}^{12}$, depending on the scenario, can come with both signs and hence increase or decrease the decay width.

4 SUSY-QCD Corrections

The SUSY-QCD corrections for the NMSSM pseudoscalar A_i decay width differ from the ones of the MSSM [39–41] solely in the tree-level coupling to the stops $G_{A_i}^{12}$. We shortly repeat them here for completeness and in order to introduce our renormalization scheme.

The virtual corrections at order $\mathcal{O}(\alpha_s)$ to the pseudoscalar Higgs decays into stops consist of loop diagrams with a gluon, respectively, gluino exchanged in the $A_i \tilde{t}_1 \tilde{t}_2$ vertex and of a contribution involving the four-squark vertex, *cf.* Fig. 1 (upper). Note that the mixing contributions due to off-diagonal self-energies are absent in the case of pseudoscalar Higgs decays, as A_i only couples to different stop mass eigenstates. The computation of the virtual diagrams leads to ultraviolet (UV) and infrared (IR) divergences. We work in dimensional reduction [78], which preserves SUSY at the one-loop level. The fields and couplings are then treated in 4 dimensions while the loop integral is performed in $D = 4 - 2\epsilon$ dimensions. The UV divergences appear as poles in ϵ and are canceled by the wave function counterterms and the counterterm renormalizing the $A_i \tilde{t}_1 \tilde{t}_2$ interaction. The infrared divergences are regularized by the introduction of a

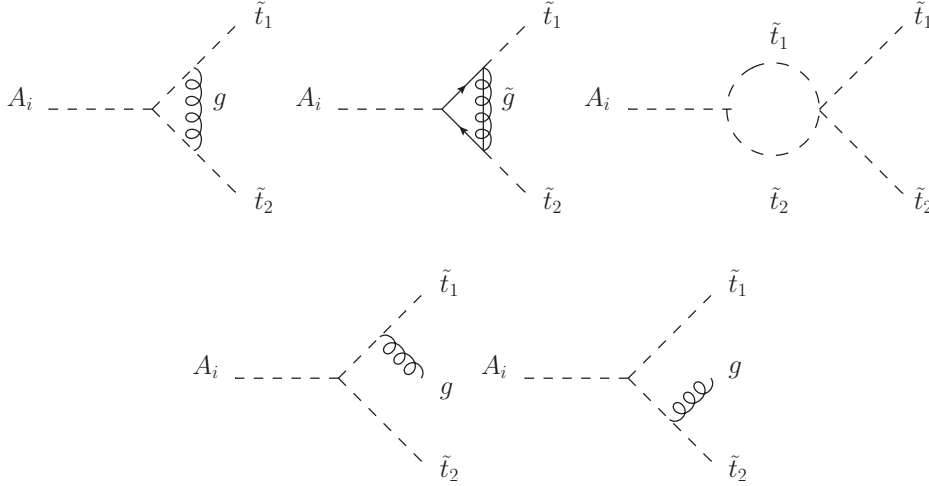


Figure 1: Diagrams contributing at NLO SUSY-QCD to the virtual (upper row) and real corrections (lower row) of the decay $\Gamma(A_i \rightarrow \tilde{t}_1 \tilde{t}_2)$.

fictitious gluon mass ζ . The IR divergences left over after renormalization are canceled after adding the real corrections. These consist of the radiation of an additional gluon off the final state stops and are shown in Fig. 1 (lower).

The one-loop corrected decay amplitude can be written as

$$\Gamma_{\text{QCD}}^{\text{NLO}} = \Gamma^{\text{LO}} + \Gamma_{\text{QCD}}^{(1)}, \quad (4.21)$$

with

$$\Gamma_{\text{QCD}}^{(1)} = \text{Re} \left[\frac{\lambda^{1/2}(M_{A_i}^2, m_{\tilde{t}_1}^2, m_{\tilde{t}_2}^2)}{4\pi M_{A_i}^3} \left(\sum_{j=1}^2 \mathbf{Z}_{ij}^* G_{A_j}^{12*} \right) \frac{\alpha_s}{\pi} \left(\sum_{k=1}^2 \mathbf{Z}_{ik} \Delta_{A_k}^{\text{QCD}} \right) \right], \quad (4.22)$$

where again the \mathbf{Z} factors appear to ensure the on-shell properties of the external loop-corrected Higgs field. The $\Delta_{A_k}^{\text{QCD}}$ are given by the sum of the virtual, real and counterterm contributions $\Delta_{A_k}^V$, $\Delta_{A_k}^R$ and $\Delta_{A_k}^{\text{CT}}$, respectively,

$$\Delta_{A_k}^{\text{QCD}} = \Delta_{A_k}^V + \Delta_{A_k}^{\text{CT}} + \Delta_{A_k}^R. \quad (4.23)$$

From now on a factor $C_F \alpha_s / (4\pi)$ with $C_F = 4/3$ is factorized out and already included in Eq. (4.22). The virtual corrections receive contributions $\Delta_{A_k}^g$ from the gluon exchange diagram, $\Delta_{A_k}^{\tilde{g}}$ from the gluino exchange diagram and $\Delta_{A_k}^{4\tilde{t}}$ from the diagram involving the 4-squark vertex. They are given by

$$\begin{aligned} \Delta_{A_k}^g &= G_{A_k}^{12} \left[B_0(m_{\tilde{t}_1}^2; \zeta, m_{\tilde{t}_1}) + B_0(m_{\tilde{t}_2}^2; \zeta, m_{\tilde{t}_2}) - B_0(M_{A_k}^2; m_{\tilde{t}_1}, m_{\tilde{t}_2}) \right. \\ &\quad \left. + 2(m_{\tilde{t}_1}^2 + m_{\tilde{t}_2}^2 - M_{A_k}^2) C_0(m_{\tilde{t}_1}^2, M_{A_k}^2, m_{\tilde{t}_2}^2; \zeta, m_{\tilde{t}_1}, m_{\tilde{t}_2}) \right] \end{aligned} \quad (4.24)$$

for the gluon exchange,

$$\begin{aligned} \Delta_{A_k}^{\tilde{g}} &= \frac{g m_t \mathcal{R}_{k1}^P}{M_W \tan \beta} \left[(m_{\tilde{g}} - m_t \sin(2\theta_{\tilde{t}})) B_0(m_{\tilde{t}_1}^2; m_{\tilde{g}}, m_t) + (m_{\tilde{g}} + m_t \sin(2\theta_{\tilde{t}})) B_0(m_{\tilde{t}_2}^2; m_{\tilde{g}}, m_t) \right. \\ &\quad \left. - (\sin(2\theta_{\tilde{t}}) m_t (m_{\tilde{t}_1}^2 - m_{\tilde{t}_2}^2) + m_{\tilde{g}} M_{A_k}^2) C_0(m_{\tilde{t}_1}^2, M_{A_k}^2, m_{\tilde{t}_2}^2; m_{\tilde{g}}, m_t, m_t) \right] \end{aligned} \quad (4.25)$$

for the gluino exchange, and

$$\Delta_{A_k}^{4\tilde{t}} = G_{A_k}^{12} B_0(M_{A_k}^2; m_{\tilde{t}_1}, m_{\tilde{t}_2}) \quad (4.26)$$

for the 4-squark vertex diagram, where B_0 and C_0 are the Passarino-Veltman scalar two- and three-point functions [79], *cf.* App. A for their definitions.

The counterterm corrections consist of the renormalization of the external squark wave functions $Z_{\tilde{t}_j\tilde{t}_j}$ ($j = 1, 2$) and the renormalization of the $A_k\tilde{t}_1\tilde{t}_2$ interaction vertex. Note that the wave function renormalization of the pseudoscalar does not contribute at order $\mathcal{O}(\alpha_s)$ and hence to the SUSY QCD corrections. The parameters λ , v , v_s , $\tan\beta$, M_W , M_Z and e are not renormalized by the strong interaction, so that the counterterm reads

$$\Delta_{A_k}^{\text{CT}} = \frac{1}{2} G_{A_k}^{12} (\delta Z_{\tilde{t}_1\tilde{t}_1} + \delta Z_{\tilde{t}_2\tilde{t}_2}) + \frac{\partial G_{A_k}^{12}}{\partial m_t} \delta m_t + \frac{\partial G_{A_k}^{12}}{\partial A_t} \delta A_t, \quad (4.27)$$

leading to

$$\Delta_{A_k}^{\text{CT}} = \frac{1}{2} G_{A_k}^{12} (\delta Z_{\tilde{t}_1\tilde{t}_1} + \delta Z_{\tilde{t}_2\tilde{t}_2}) + G_{A_k}^{12} \frac{\delta m_t}{m_t} + \frac{g m_t}{2 M_W} \frac{\mathcal{R}_{k1}^P}{\tan\beta} \delta A_t. \quad (4.28)$$

The counterterm δA_t of the trilinear coupling is given by the quark and squark mass counterterms, δm_t and $\delta m_{\tilde{t}_{1,2}}$, and the mixing angle counterterm $\delta\theta_{\tilde{t}}$,

$$\delta A_t = \frac{1}{2m_t} \left[(m_{\tilde{t}_1}^2 - m_{\tilde{t}_2}^2) \left(2 \cos(2\theta_{\tilde{t}}) \delta\theta_{\tilde{t}} - \sin(2\theta_{\tilde{t}}) \frac{\delta m_t}{m_t} \right) + 2 \sin(2\theta_{\tilde{t}}) (m_{\tilde{t}_1} \delta m_{\tilde{t}_1} - m_{\tilde{t}_2} \delta m_{\tilde{t}_2}) \right]. \quad (4.29)$$

In the (s)quark sector we adopt OS renormalization with the quark and squark masses defined as the poles of their respective propagators and the squark wave function renormalization constants defined such that the residues of the poles are equal to one. Defining the following structure for the quark self-energy, where $\mathcal{P}_{L,R}$ denote, respectively, the left- and right-chiral projector,

$$\Sigma_t(p^2) \equiv \not{p} \Sigma_t^L(p^2) \mathcal{P}_L + \not{p} \Sigma_t^R(p^2) \mathcal{P}_R + m_t \Sigma_t^{Ls}(p^2) \mathcal{P}_L + m_t \Sigma_t^{Rs}(p^2) \mathcal{P}_R, \quad (4.30)$$

we have for the top quark mass counterterm

$$\delta m_t = \frac{1}{2} \text{Re} \left(m_t \Sigma_t^L(m_t^2) + m_t \Sigma_t^R(m_t^2) + \Sigma_t^{Ls}(m_t^2) + \Sigma_t^{Rs}(m_t^2) \right). \quad (4.31)$$

The squark mass and wave function counterterms are given by ($j = 1, 2$)

$$\delta m_{\tilde{t}_j}^2 = \text{Re} \Sigma_{\tilde{t}_j\tilde{t}_j}(m_{\tilde{t}_j}^2) \quad (4.32)$$

$$\delta Z_{\tilde{t}_j\tilde{t}_j} = -\text{Re} \left. \frac{\partial \Sigma_{\tilde{t}_j\tilde{t}_j}(p^2)}{\partial p^2} \right|_{p^2=m_{\tilde{t}_j}^2}. \quad (4.33)$$

In Eq. (4.32) the $\Sigma_{\tilde{t}_j\tilde{t}_j}$ denote the diagonal parts of the squark self-energies. The diagrams contributing at order $\mathcal{O}(\alpha_s)$ to the squark and quark self-energies are depicted in Fig. 2 (upper) and (lower), respectively.

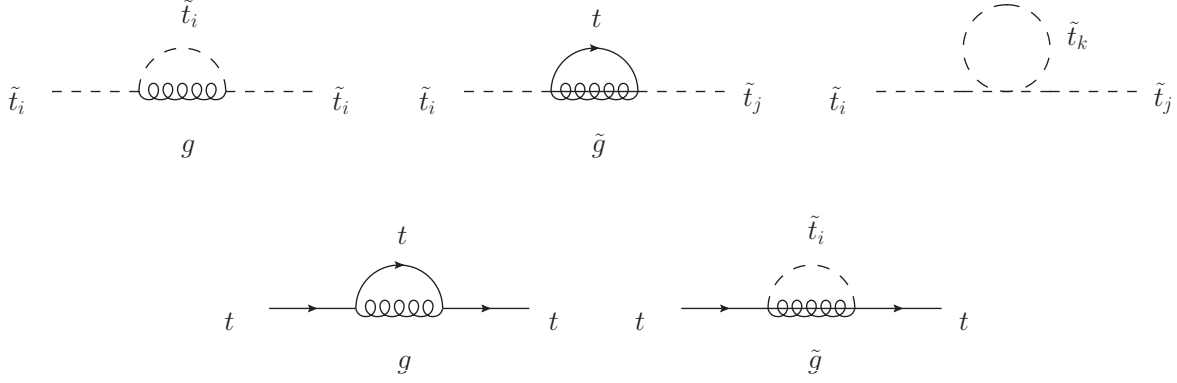


Figure 2: Diagrams contributing at NLO SUSY-QCD to the squark self-energies (upper row) and to the quark self-energies (lower row).

The mass counterterms read

$$\begin{aligned} \frac{\delta m_t}{m_t} = & -\text{Re} \left[2B_1(m_t^2; m_t, \zeta) + B_1(m_t^2; m_{\tilde{g}}, m_{\tilde{t}_1}) + B_1(m_t^2; m_{\tilde{g}}, m_{\tilde{t}_2}) + 4B_0(m_t^2; m_t, \zeta) \right. \\ & \left. + \sin(2\theta_{\tilde{t}}) \frac{m_{\tilde{g}}}{m_t} (B_0(m_t^2; m_{\tilde{g}}, m_{\tilde{t}_1}) - B_0(m_t^2; m_{\tilde{g}}, m_{\tilde{t}_2})) \right] \end{aligned} \quad (4.34)$$

$$\begin{aligned} m_{\tilde{t}_1} \delta m_{\tilde{t}_1} = & \text{Re} \left[2m_t m_{\tilde{g}} \sin(2\theta_{\tilde{t}}) B_0(m_{\tilde{t}_1}^2; m_t, m_{\tilde{g}}) + \frac{1}{2} [(1 + \cos^2(2\theta_{\tilde{t}})) A_0(m_{\tilde{t}_1}) \right. \\ & \left. + \sin^2(2\theta_{\tilde{t}}) A_0(m_{\tilde{t}_2})] - 2m_{\tilde{t}_1}^2 B_0(m_{\tilde{t}_1}^2; m_{\tilde{t}_1}, \zeta) - A_0(m_{\tilde{g}}) - A_0(m_t) \right. \\ & \left. + (m_{\tilde{t}_1}^2 - m_t^2 - m_{\tilde{g}}^2) B_0(m_{\tilde{t}_1}^2; m_t, m_{\tilde{g}}) \right] \end{aligned} \quad (4.35)$$

$$\begin{aligned} m_{\tilde{t}_2} \delta m_{\tilde{t}_2} = & \text{Re} \left[-2m_t m_{\tilde{g}} \sin(2\theta_{\tilde{t}}) B_0(m_{\tilde{t}_2}^2; m_t, m_{\tilde{g}}) + \frac{1}{2} [(1 + \cos^2(2\theta_{\tilde{t}})) A_0(m_{\tilde{t}_2}) \right. \\ & \left. + \sin^2(2\theta_{\tilde{t}}) A_0(m_{\tilde{t}_1})] - 2m_{\tilde{t}_2}^2 B_0(m_{\tilde{t}_2}^2; m_{\tilde{t}_2}, \zeta) - A_0(m_{\tilde{g}}) - A_0(m_t) \right. \\ & \left. + (m_{\tilde{t}_2}^2 - m_t^2 - m_{\tilde{g}}^2) B_0(m_{\tilde{t}_2}^2; m_t, m_{\tilde{g}}) \right], \end{aligned} \quad (4.36)$$

where B_1 is the coefficient of the two-point tensor integral of rank one and A_0 denotes the scalar one-point function, *cf.* App. A. The wave function corrections can be cast into the form

$$\begin{aligned} \delta Z_{\tilde{t}_1 \tilde{t}_1} = & \text{Re} \left[-4m_t m_{\tilde{g}} \sin(2\theta_{\tilde{t}}) B'_0(m_{\tilde{t}_1}^2; m_t, m_{\tilde{g}}) + 2(m_{\tilde{g}}^2 + m_t^2 - m_{\tilde{t}_1}^2) B'_0(m_{\tilde{t}_1}^2; m_t, m_{\tilde{g}}) \right. \\ & \left. + 2B_0(m_{\tilde{t}_1}^2; m_{\tilde{t}_1}, \zeta) - 2B_0(m_{\tilde{t}_1}^2; m_t, m_{\tilde{g}}) + 4m_{\tilde{t}_1}^2 B'_0(m_{\tilde{t}_1}^2; m_{\tilde{t}_1}, \zeta) \right] \end{aligned} \quad (4.37)$$

$$\begin{aligned} \delta Z_{\tilde{t}_2 \tilde{t}_2} = & \text{Re} \left[4m_t m_{\tilde{g}} \sin(2\theta_{\tilde{t}}) B'_0(m_{\tilde{t}_2}^2; m_t, m_{\tilde{g}}) + 2(m_{\tilde{g}}^2 + m_t^2 - m_{\tilde{t}_2}^2) B'_0(m_{\tilde{t}_2}^2; m_t, m_{\tilde{g}}) \right. \\ & \left. + 2B_0(m_{\tilde{t}_2}^2; m_{\tilde{t}_2}, \zeta) - 2B_0(m_{\tilde{t}_2}^2; m_t, m_{\tilde{g}}) + 4m_{\tilde{t}_2}^2 B'_0(m_{\tilde{t}_2}^2; m_{\tilde{t}_2}, \zeta) \right]. \end{aligned} \quad (4.38)$$

Here $B'_0(k^2; m_1^2, m_2^2)$ denotes the derivative with respect to k^2 . The mixing angle counterterm is renormalized as

$$\delta\theta_{\tilde{t}} = \frac{1}{2} (\delta Z_{\tilde{t}_1 \tilde{t}_2} - \delta Z_{\tilde{t}_2 \tilde{t}_1}) = \frac{1}{2(m_{\tilde{t}_1}^2 - m_{\tilde{t}_2}^2)} \text{Re} [\Sigma_{\tilde{t}_1 \tilde{t}_2}(m_{\tilde{t}_2}^2) + \Sigma_{\tilde{t}_2 \tilde{t}_1}(m_{\tilde{t}_1}^2)], \quad (4.39)$$

where $\Sigma_{\tilde{t}_i \tilde{t}_j}$ denotes the respective squark self-energies, so that

$$\begin{aligned} \delta\theta_{\tilde{t}} = & \frac{1}{m_{\tilde{t}_1}^2 - m_{\tilde{t}_2}^2} \text{Re} \left[\sin(2\theta_{\tilde{t}}) \cos(2\theta_{\tilde{t}}) \left(A_0(m_{\tilde{t}_2}^2) - A_0(m_{\tilde{t}_1}^2) \right) \right. \\ & \left. + 2m_t m_{\tilde{g}} \cos(2\theta_{\tilde{t}}) \left(B_0(m_{\tilde{t}_2}^2; m_t, m_{\tilde{g}}) + B_0(m_{\tilde{t}_1}^2; m_t, m_{\tilde{g}}) \right) \right] . \end{aligned} \quad (4.40)$$

The real corrections finally in terms of dilogarithms read

$$\begin{aligned} \Delta_{A_k}^R = & \frac{2G_{A_k}^{12}}{\lambda^{1/2}} \left[(M_{A_k}^2 - m_{\tilde{t}_1}^2 - m_{\tilde{t}_2}^2) \left(-2 \log \beta_0 \log \frac{\zeta M_{A_k} m_{\tilde{t}_1} m_{\tilde{t}_2}}{\lambda} + 2 \log^2 \beta_0 \right. \right. \\ & - \log^2 \beta_1 - \log^2 \beta_2 + 2 \text{Li}_2(1 - \beta_0^2) - \text{Li}_2(1 - \beta_1^2) - \text{Li}_2(1 - \beta_2^2) \Big) \\ & + 2\lambda^{1/2} \log \frac{\zeta M_{A_k} m_{\tilde{t}_1} m_{\tilde{t}_2}}{\lambda} + 4\lambda^{1/2} + (2M_{A_k}^2 + m_{\tilde{t}_1}^2 + m_{\tilde{t}_2}^2) \log \beta_0 \\ & \left. + (M_{A_k}^2 + 2m_{\tilde{t}_2}^2) \log \beta_2 + (M_{A_k}^2 + 2m_{\tilde{t}_1}^2) \log \beta_1 \right] , \end{aligned} \quad (4.41)$$

where in the two-body phase space function $\lambda(M_{A_k}^2, m_{\tilde{t}_1}^2, m_{\tilde{t}_2}^2)$ we have neglected the arguments for better readability. We have furthermore introduced

$$\begin{aligned} \beta_0 &= \frac{M_{A_k}^2 - m_{\tilde{t}_1}^2 - m_{\tilde{t}_2}^2 + \lambda^{1/2}}{2m_{\tilde{t}_1} m_{\tilde{t}_2}} \\ \beta_1 &= \frac{M_{A_k}^2 - m_{\tilde{t}_1}^2 + m_{\tilde{t}_2}^2 - \lambda^{1/2}}{2M_{A_k} m_{\tilde{t}_2}} \\ \beta_2 &= \frac{M_{A_k}^2 + m_{\tilde{t}_1}^2 - m_{\tilde{t}_2}^2 - \lambda^{1/2}}{2M_{A_k} m_{\tilde{t}_1}} . \end{aligned} \quad (4.42)$$

5 The One-Loop Electroweak Corrections

The NLO electroweak corrections consist of the virtual corrections to the vertex and the counterterm contributions to cancel the UV divergences. Besides the top and stop fields and the parameters specified below, again the Higgs field needs to be renormalized, as for the external Higgs field we use the two-loop corrected Higgs boson mass at order $\mathcal{O}(\alpha_t \alpha_s)$, including the full EW corrections at one-loop order. In the loops, however, the tree-level masses for the Higgs bosons have to be used so that the UV divergences are canceled properly.

For the NLO EW corrections, in addition the mixings

$$\delta M_{\text{mix},i}^{G,Z} \equiv \delta M_{\text{mix},i}^{G,Z}(A_i \rightarrow \tilde{t}_1 \tilde{t}_2) \quad (5.43)$$

of the decaying CP-odd Higgs boson A_i with the Z boson and the Goldstone boson G have to be included. The matrix element for the EW corrected pseudoscalar Higgs decay into stops hence reads

$$\mathcal{M}(A_i \rightarrow \tilde{t}_1 \tilde{t}_2) = \sum_{j=1}^2 \mathbf{z}_{ij} \left(-G_{A_j}^{12} + \Delta_{A_j}^{\text{EW}} \right) + \delta M_{\text{mix},i}^{G,Z} , \quad (5.44)$$

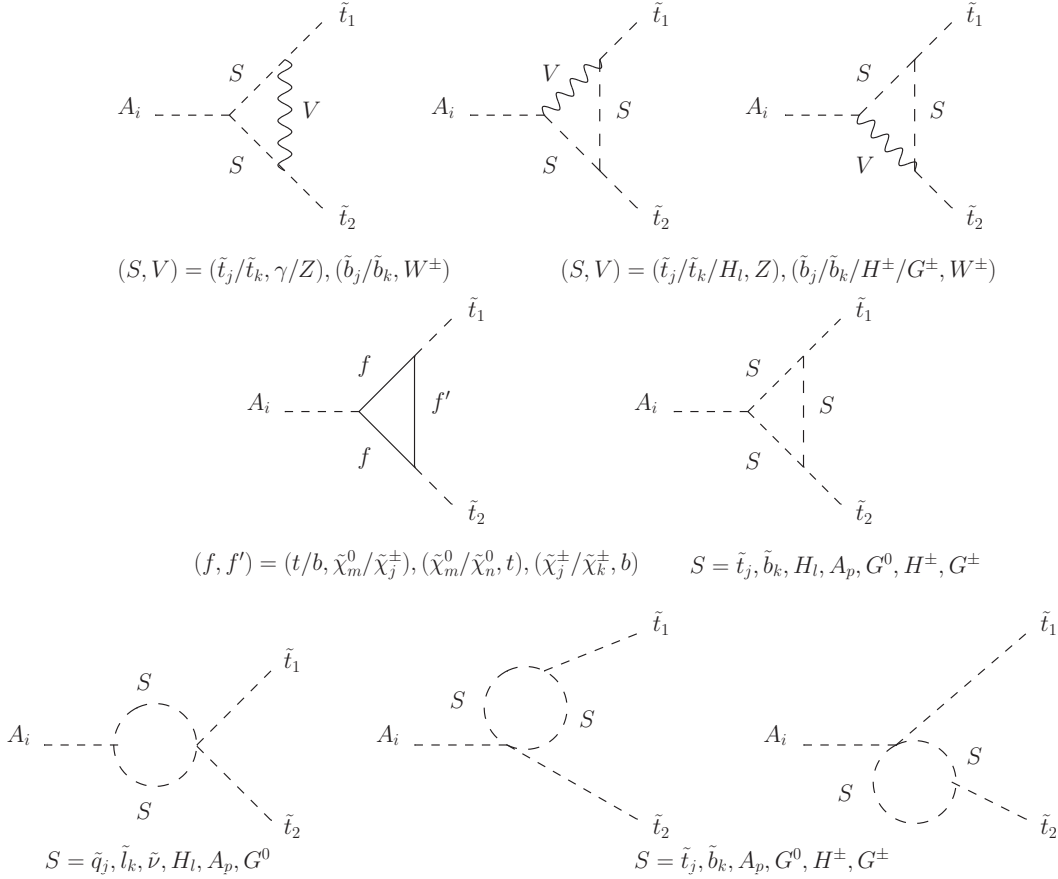


Figure 3: Generic diagrams contributing to the electroweak corrections of the decay $\Gamma(A_i \rightarrow \tilde{t}_1 \tilde{t}_2)$ with $i, j, k, p = 1, 2, l = 1, 2, 3$ and $m, n = 1, \dots, 5$.

where $\Delta_{A_j}^{\text{EW}}$ represents the sum of the 1-particle irreducible (1PI) diagrams $\Delta_{A_j}^{V,\text{EW}}$ contributing to the EW virtual corrections of the vertex and of the counterterms $\Delta_{A_j}^{\text{CT,EW}}$,

$$\Delta_{A_j}^{\text{EW}} = \Delta_{A_j}^{V,\text{EW}} + \Delta_{A_j}^{\text{CT,EW}}. \quad (5.45)$$

Due to massless photons in the loops we also encounter IR divergences. These are canceled by adding the real corrections $\Delta^{R,\text{EW}}$, where a photon is radiated off the final state stop lines. We hence have for the EW corrected decay amplitude

$$\Gamma_{\text{EW}}^{\text{NLO}}(A_i \rightarrow \tilde{t}_1 \tilde{t}_2) = \frac{3\lambda^{1/2}}{8\pi M_{A_i}^3} \left[\left| \sum_{j=1}^2 \mathbf{z}_{ij} G_{A_j}^{12} \right|^2 + \left(\sum_{j=1}^2 \mathbf{z}_{ij}^* G_{A_j}^{12*} \right) \left(\sum_{k=1}^2 \mathbf{z}_{ik} \Delta_{A_k}^{R,\text{EW}} \right) - 2\text{Re} \left(\sum_{j=1}^2 \mathbf{z}_{ij}^* G_{A_j}^{12*} \left(\sum_{k=1}^2 \mathbf{z}_{ik} \Delta_{A_k}^{\text{EW}} + \delta M_{\text{mix},i}^{G,Z} \right) \right) \right]. \quad (5.46)$$

Again we have dropped the arguments in the two-body phase space function λ . In the following we will discuss the individual contributions. The virtual corrections consist of the 1PI diagrams given by the triangle diagrams with scalars, fermions and gauge bosons in the loops, as shown in

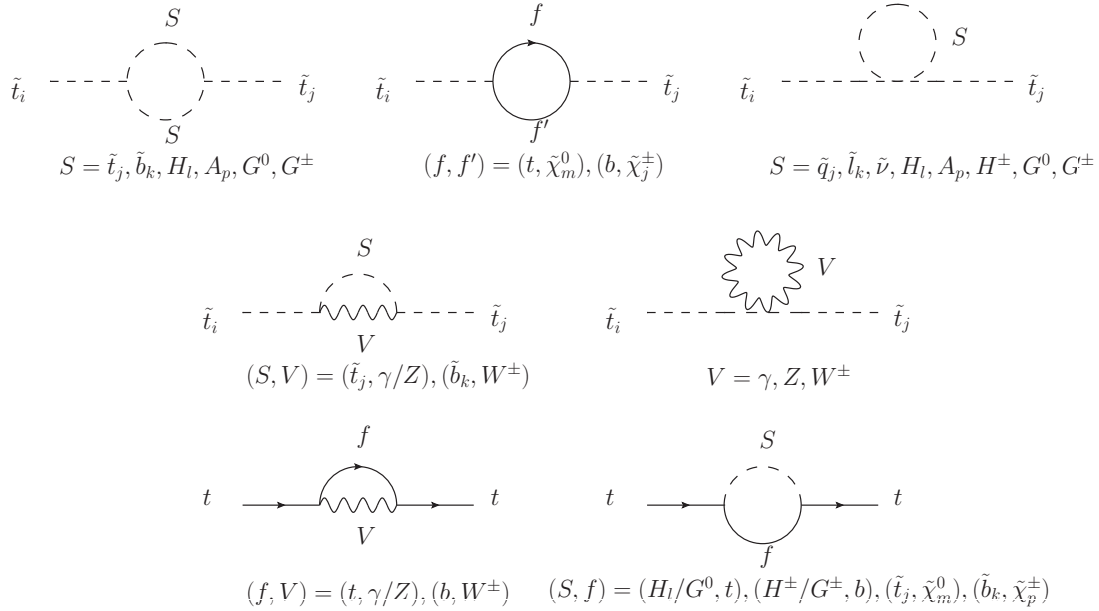


Figure 4: Diagrams contributing to the electroweak squark self-energies (first two rows) and quark self-energies (last row) with $i, j, k, p = 1, 2$, $l = 1, 2, 3$ and $m = 1, \dots, 5$.

the first two rows of Fig. 3, and of the diagrams involving four-particle vertices, *cf.* Fig. 3 (last row). For better readability, for the scalars S appearing in the loops we only listed the particle types but not the combination of scalars that are allowed by the theory for the various vertices. Let us remark, however, that in the four-particle vertices the scalar-Higgs-Goldstone-boson-2-stops coupling $H_l - G - \tilde{t}_1 - \tilde{t}_2$ and the scalar-pseudoscalar-2-stops coupling $H_l - A_p - \tilde{t}_1 - \tilde{t}_2$ ($l = 1, 2, 3$, $p = 1, 2$) are new compared to the MSSM. The former is due to the singlet admixture in H_l , the latter is proportional to the NMSSM specific coupling λ . The diagrams have been generated with the Mathematica package **FeynArts** 3.6 [80] and evaluated with **FormCalc** 7.3 [81] in two independent calculations. The integrals have been computed with **LoopTools** 2.7 [81]. The results of both calculations agree and have been cross-checked against a third calculation, that did not use any of the tools to evaluate and simplify the amplitudes, and which takes the loop functions from **HDECAY** [82, 83] and **SDECAY** [84]. The UV divergences encountered in the computation of the virtual corrections are canceled by the counterterms that are the sum of the stop wave function corrections and of the counterterm renormalizing the $A_j \tilde{t}_1 \tilde{t}_2$ interaction,

$$\Delta_{A_j}^{\text{CT,EW}} = \Delta_{A_j}^{\text{CT},w} + \Delta_{A_j}^{\text{CT},v} \quad (5.47)$$

Because of the antisymmetric $G_{A_j}^{12}$ coupling the stop wave function corrections are given by

$$\Delta_{A_j}^{\text{CT},w} = -\frac{G_{A_j}^{12}}{2} (\delta Z_{\tilde{t}_1 \tilde{t}_1} + \delta Z_{\tilde{t}_2 \tilde{t}_2}) . \quad (5.48)$$

The stops are renormalized on-shell, with the renormalization conditions given in Eqs. (4.32) and (4.33). The diagrams, that contribute to the here required electroweak self-energies are displayed in Fig. 4 (upper two rows).

For the one-loop EW corrections the vertex counterterm reads

$$\begin{aligned} \Delta_{A_j}^{\text{CT},v} = & -G_{A_j}^{12} \left(\frac{\delta g}{g} + \frac{\delta m_t}{m_t} - \frac{\delta M_W}{M_W} \right) - \frac{gm_t}{2M_W} \left[\mathcal{R}_{j1}^P \left(\delta\mu + \left(\frac{\delta A_t}{A_t} - \frac{\delta \tan \beta}{\tan \beta} \right) \frac{A_t}{\tan \beta} \right) \right. \\ & \left. + \left(\frac{\delta \lambda}{\lambda} + \frac{\delta v}{v} - \frac{\delta \tan \beta}{\tan \beta} \right) \frac{\lambda v}{\sqrt{2} \tan \beta} \mathcal{R}_{j2}^P \right]. \end{aligned} \quad (5.49)$$

The individual counterterms are derived from the renormalization of the input parameters. We follow Ref. [56] and apply the same renormalization scheme which mixes OS and $\overline{\text{DR}}$ conditions as defined there. For the vertex counterterms the relevant input parameters are the W and Z boson masses M_W and M_Z , the electric charge e , $\tan \beta$, λ and v_s .² The parameters that can be related to physical quantities are renormalized OS, the remaining ones $\overline{\text{DR}}$. Together with the OS-renormalized top/stop sector, we have the following set of parameters to be renormalized,

$$\underbrace{\tan \beta, \lambda, v_s}_{\overline{\text{DR}} \text{ scheme}}, \underbrace{M_Z, M_W, e, m_t, m_{\tilde{t}_1}, m_{\tilde{t}_2}, \theta_{\tilde{t}}}_{\text{OS scheme}}. \quad (5.50)$$

The coupling g and the VEV v appearing in Eq. (5.49) are given in terms of these parameters by

$$g = \frac{eM_Z}{\sqrt{M_Z^2 - M_W^2}} \quad \text{and} \quad v = \frac{2M_W}{e} \sqrt{1 - \frac{M_W^2}{M_Z^2}}, \quad (5.51)$$

from which their counterterms can be derived. The details of the renormalization of the counterterms for the first six input parameters can be found in [56], so that they are not repeated here. The formulae for the OS renormalization of the top and stop masses are given in Eqs. (4.31)-(4.33). The squark and quark self-energies for the EW one-loop corrections are depicted in Fig. 4. At EW one-loop order the counterterm for A_t now reads

$$\begin{aligned} \delta A_t = & \frac{\mu}{\tan \beta} \left(\frac{\delta \mu}{\mu} - \frac{\delta \tan \beta}{\tan \beta} \right) + \frac{1}{2m_t} \left[(m_{\tilde{t}_1}^2 - m_{\tilde{t}_2}^2) \left(2\delta\theta_{\tilde{t}} \cos(2\theta_{\tilde{t}}) - \sin(2\theta_{\tilde{t}}) \frac{\delta m_t}{m_t} \right) \right. \\ & \left. + 2\sin(2\theta_{\tilde{t}})(m_{\tilde{t}_1} \delta m_{\tilde{t}_1} - m_{\tilde{t}_2} \delta m_{\tilde{t}_2}) \right]. \end{aligned} \quad (5.52)$$

The counterterm for the mixing angle $\theta_{\tilde{t}}$ is renormalized as in Eq. (4.39), however with the self-energies given by the diagrams shown in Fig. 4 (first two rows).

The diagrams for the contributions to the electroweak corrections stemming from the mixings of the pseudoscalar A_i with the Z boson and the Goldstone boson, $\delta M_{\text{mix},i}^{G,Z}$, are shown in Fig. 5. Using the Slavnov-Taylor identity [85], one can obtain the mixing contributions through

$$\delta M_{\text{mix},i}^{G,Z} = \frac{G_G^{12}}{M_Z} \hat{\Sigma}_{A_i Z} \left((M_{A_i}^{(0)})^2 \right), \quad (5.53)$$

where $\hat{\Sigma}_{A_i Z}$ denotes the renormalized A_i - Z mixing self-energy and G_G^{12} is the Goldstone boson coupling to the stops,

$$G_G^{12} = -\frac{gm_t}{2M_W} \left(A_t - \frac{\mu}{\tan \beta} \right). \quad (5.54)$$

²Additionally, for the renormalization of the Higgs sector in the computation of the higher order corrections to the Higgs boson masses, we have the tadpole parameters, the mass of the charged Higgs boson M_{H^\pm} , the NMSSM parameter κ and the trilinear coupling A_κ , which need to be renormalized at loop level, *cf.* [56].

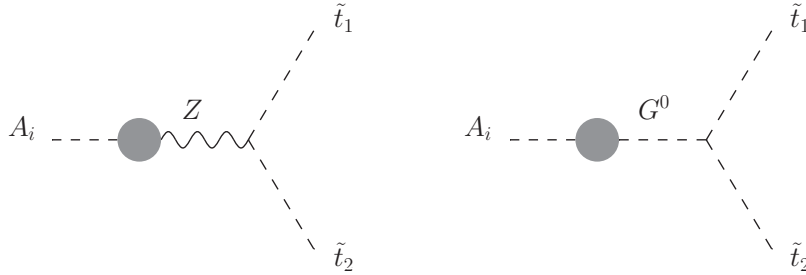


Figure 5: Generic one-loop diagrams contributing to the mixing $\delta M_{\text{mix},i}^{G,Z}$ of a pseudoscalar A_i with the Z and Goldstone boson.

Note, in particular that the external momenta have to be set to the tree-level mass $M_{A_i}^{(0)}$ in order to ensure to maintain gauge invariance.

The last piece which is missing in the decay, in order to also get an IR finite result, is the real corrections term $\Delta_{A_k}^{R,\text{EW}}$. This is the same as for the QCD corrections, but with the gluon replaced by the photon. In the formula for the QCD corrections, Eq. (4.41), this means that the coupling and color factors have to be replaced accordingly, *i.e.*

$$\Delta_{A_k}^{R,\text{EW}} = \frac{e^2}{16\pi^2} \Delta_{A_k}^R, \quad (5.55)$$

with $\Delta_{A_k}^R$ given in Eq. (4.41).

The full NLO decay width including the SUSY-QCD and -EW corrections is then given by

$$\Gamma^{\text{NLO, full}} = \Gamma_{\text{EW}}^{\text{NLO}} + \Gamma_{\text{QCD}}^{(1)}, \quad (5.56)$$

where $\Gamma_{\text{EW}}^{\text{NLO}}$, defined in Eq. (5.46), includes the leading order decay width and $\Gamma_{\text{QCD}}^{(1)}$ has been defined in Eq. (4.21).

6 Numerical Analysis

For our numerical analysis we first perform a scan in the NMSSM parameter space in order to find scenarios that are in accordance with the LHC Higgs and SUSY data. The compatibility with the LHC Higgs data has been checked by using the programs **HiggsBounds** [86] and **HiggsSignals** [87]. The effective couplings of the NMSSM Higgs bosons, normalized to the corresponding SM values, as well as the masses, the widths and the branching ratios of the NMSSM Higgs bosons, which are required as inputs for these programs, have been obtained from the Fortran code **NMSSMCALC** [73]. The loop induced Higgs coupling to gluons normalized to the corresponding coupling of a SM Higgs boson with same mass is obtained by taking the ratio of the partial widths for the Higgs decays into gluons in the NMSSM and the SM, respectively. These include the QCD corrections up to next-to-next-to-next-to leading order in the limit of heavy quarks [88–97] and squarks [98,99], taken over from the SM, respectively, MSSM case, while the EW are unknown for the SUSY case and hence consistently neglected also in the SM decay width. The stop mass values have been chosen such that they are not excluded by present ATLAS [100–102] and CMS [103,104] searches. The squark masses of the first two generation are heavy enough not to

be in conflict with LHC data. The SM input parameters that we use are [105, 106]

$$\begin{aligned} \alpha(M_Z) &= 1/128.962, & \alpha_s^{\overline{\text{MS}}}(M_Z) &= 0.1184, & M_Z &= 91.1876 \text{ GeV}, \\ M_W &= 80.385 \text{ GeV}, & m_t &= 173.5 \text{ GeV}, & m_b^{\overline{\text{MS}}}(m_b^{\overline{\text{MS}}}) &= 4.19 \text{ GeV}. \end{aligned} \quad (6.57)$$

The running $\alpha_s^{\overline{\text{DR}}}$ used in `NMSSMCALC` is obtained by converting the $\alpha_s^{\overline{\text{MS}}}$, that is evaluated with the SM renormalization group equations at two-loop order, to the $\overline{\text{DR}}$ scheme. The light quark masses, which have only a small influence on the loop results, have been set to

$$m_u = 2.5 \text{ MeV}, \quad m_d = 4.95 \text{ MeV}, \quad m_s = 100 \text{ MeV} \quad \text{and} \quad m_c = 1.42 \text{ GeV}. \quad (6.58)$$

As renormalization scale μ_R we choose the SUSY scale M_s , which we set

$$M_s = \sqrt{m_{\tilde{Q}_3} m_{\tilde{t}_R}} = \mu_R. \quad (6.59)$$

6.1 Pseudoscalar Higgs Boson Decays into Stop Pairs

In this subsection we present the impact of the SUSY-QCD and -EW corrections on the decay of a heavy pseudoscalar Higgs boson into a pair of stop quarks. The parameter point, which we have chosen from the set of parameter points that survive the LHC constraints, is given by the soft SUSY breaking masses and trilinear couplings

$$\begin{aligned} m_{\tilde{u}_R, \tilde{c}_R} &= m_{\tilde{d}_R, \tilde{s}_R} = m_{\tilde{Q}_{1,2}} = m_{\tilde{L}_{1,2}} = m_{\tilde{e}_R, \tilde{\mu}_R} = 3 \text{ TeV}, \quad m_{\tilde{t}_R} = 536.43 \text{ GeV}, \\ m_{\tilde{Q}_3} &= 594.61 \text{ GeV}, \quad m_{\tilde{b}_R} = 1285 \text{ GeV}, \quad m_{\tilde{L}_3} = 255.53 \text{ GeV}, \quad m_{\tilde{\tau}_R} = 1499 \text{ GeV}, \\ A_t &= 1418 \text{ GeV}, \quad A_{u,c} = 1435 \text{ GeV}, \quad A_{d,s,b} = -66.68 \text{ GeV}, \quad A_{e,\mu,\tau} = -91.76 \text{ GeV}, \\ M_1 &= 111.73 \text{ GeV}, \quad M_2 = 395.86 \text{ GeV}, \quad M_3 = 1370 \text{ GeV} \end{aligned} \quad (6.60)$$

and NMSSM specific input parameters

$$\begin{aligned} \lambda &= 0.629, \quad \kappa = 0.223, \quad A_\kappa = -543.53 \text{ GeV}, \quad \mu_{\text{eff}} = 452.61 \text{ GeV}, \\ \tan \beta &= 1.969, \quad M_{H^\pm} = 1024 \text{ GeV}. \end{aligned} \quad (6.61)$$

This results in the two-loop corrected mass M_{A_2} of the heavy pseudoscalar A_2 and the stop masses $m_{\tilde{t}_{1,2}}$,

$$M_{A_2} = 1012 \text{ GeV}, \quad m_{\tilde{t}_1} = 280.78 \text{ GeV} \quad \text{and} \quad m_{\tilde{t}_2} = 709.07 \text{ GeV}. \quad (6.62)$$

We follow the SLHA format [107], in which the parameters $\lambda, \kappa, A_\kappa, \mu_{\text{eff}}, \tan \beta$ as well as the soft SUSY breaking masses and trilinear couplings are understood as $\overline{\text{DR}}$ parameters at the scale $\mu_R = M_s$ ³, whereas the charged Higgs mass is an OS parameter. As input for our computation we take the soft SUSY breaking trilinear stop coupling A_t , however, consistently as OS parameter. The conversion from the $\overline{\text{DR}}$ to the OS scheme is done within `NMSSMCALC` and yields⁴

$$A_t^{\text{OS}} = 1435 \text{ GeV}. \quad (6.63)$$

³For $\tan \beta$ this is the case only, if it is read in from the block `EXTPAR`. Otherwise it is the $\overline{\text{DR}}$ parameter at the scale M_Z .

⁴Note, however, that the conversion is done through a counterterm that involves, as required for the order $\mathcal{O}(\alpha_t \alpha_s)$ corrections computed in `NMSSMCALC` order $\mathcal{O}(\alpha_s)$ corrections and no EW corrections.

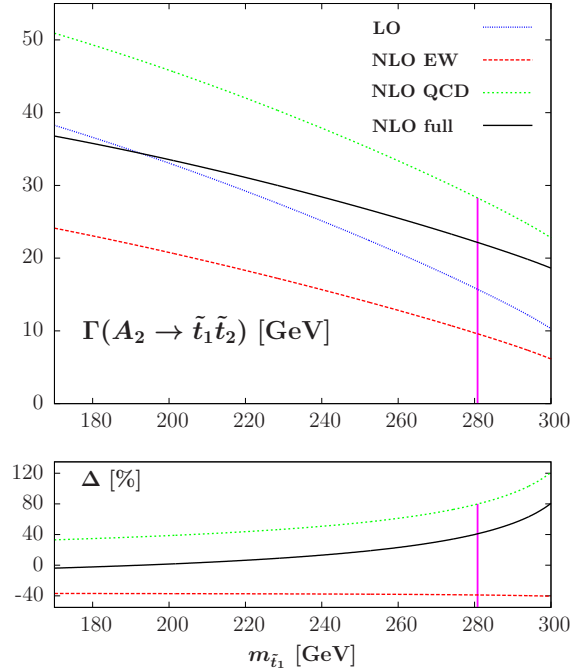


Figure 6: Upper: The partial decay width $\Gamma(A_2 \rightarrow \tilde{t}_1 \tilde{t}_2)$ as a function of $m_{\tilde{t}_1}$ at LO (blue/lower dotted), including the NLO QCD (green/upper dotted), the NLO EW (red/dashed) and both the EW and QCD corrections (black/full). Lower: The relative correction $\Delta = (\Gamma_X^{\text{NLO}} - \Gamma^{\text{LO}})/\Gamma^{\text{LO}}$ in per cent for $X = \text{QCD}$ (green/dotted), EW (red/dashed) and the full NLO corrections (black/full). The pink line shows the position of the parameter point defined in Eqs. (6.57)–(6.61).

The leading order width obtained in this scenario amounts to

$$\Gamma^{\text{LO}}(A_2 \rightarrow \tilde{t}_1 \tilde{t}_2) = 15.72 \text{ GeV} , \quad (6.64)$$

where again we have summed over both charge conjugated stop pair final states. The LO width differs by 2.7% from the value obtained at tree level with NMSSMCALC, where the Fermi constant G_F instead of α is used as input parameter.

In Fig. 6 (upper) we show the partial decay width $\Gamma(A_2 \rightarrow \tilde{t}_1 \tilde{t}_2)$ at LO, including the EW and the QCD corrections, and the NLO width with both the QCD and EW corrections taken into account, as a function of $m_{\tilde{t}_1}$, which is varied around the parameter point defined in Eqs. (6.57)–(6.61) with $m_{\tilde{t}_1} \approx 281 \text{ GeV}$.⁵ Note, that stops can still be rather light [101, 102, 104, 108, 109], down to about 240 GeV for arbitrary neutralino masses [102] and even lower taking into account the actual \tilde{t}_1 branching ratio [109]. The figure illustrates the effect of the higher order corrections, although the thus obtained parameter configurations are not all in accordance with the applied constraints anymore. The lower plot displays the relative corrections

$$\Delta = \frac{\Gamma_X^{\text{NLO}} - \Gamma^{\text{LO}}}{\Gamma^{\text{LO}}} , \quad X = \text{QCD}, \text{EW}, \text{QCD+EW} \quad (6.65)$$

in per cent. The plots show that both the QCD and the EW corrections are significant and come with opposite sign. The QCD correction increase the LO width by $\sim 40 - 120\%$ in the

⁵The variation of $m_{\tilde{t}_1}$ between 170 and 300 GeV corresponds to a variation of A_t^{OS} between 1371 and 1721 GeV.

investigated range, depending on the value of $m_{\tilde{t}_1}$, whereas the EW corrections are almost independent of $m_{\tilde{t}_1}$ and decrease the cross section by 40%. At $m_{\tilde{t}_1} = 192$ GeV the QCD and EW corrections are of same size and cancel each other. The full corrections hence increase the width between $\sim 0 - 80\%$, *cf.* Fig. 6 (lower). And for our parameter point the total correction is

$$\Delta\Gamma^{\text{QCD+EW}}(A_2 \rightarrow \tilde{t}_1\tilde{t}_2) = 41\% . \quad (6.66)$$

This plot demonstrates that both the inclusion of the EW and the QCD corrections is required in order to properly predict the decay width.

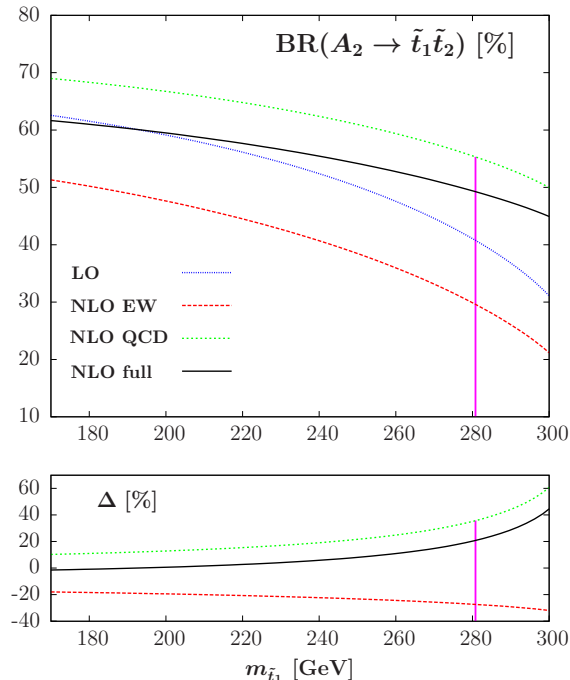


Figure 7: Same as Fig. 6, but for the branching ratios.

In Fig. 7 we show the branching ratios corresponding to the widths of Fig. 6. They have been obtained by replacing in `NMSSMCALC` the corresponding width with our loop corrected width.⁶ The branching ratio at LO of our investigated parameter point amounts to

$$\text{BR}^{\text{LO}}(A_2 \rightarrow \tilde{t}_1\tilde{t}_2) = 40.8\% . \quad (6.67)$$

The net effect of the NLO EW and QCD corrections is an increase of the branching ratio by

$$\Delta\text{BR}^{\text{QCD+EW}}(A_2 \rightarrow \tilde{t}_1\tilde{t}_2) = 20.8\% . \quad (6.68)$$

In the plot of Fig. 7 we again vary $m_{\tilde{t}_1}$ around the chosen parameter point, illustrated by the pink line in the plot. As can be read off the lower plot the total NLO corrections increase the

⁶In `NMSSMCALC` the SUSY QCD corrections to the decays into squarks, as derived from [42], are taken into account. These include improvements in the decays into sbottoms, which are required in parts of the parameter space, that are not relevant for us. Furthermore, we include the EW corrections. We therefore consistently turned off the corrections implemented in `NMSSMCALC` in the decays into squarks and included instead our corrections.

branching ratio by up to a bit more than 40% in the shown $m_{\tilde{t}_1}$ range. Thus this decay remains the most important one also after inclusion of the NLO corrections.

Figure 8 finally shows the dependence of the higher order corrections on the gluino mass. The EW corrections of course do not depend on $m_{\tilde{g}}$, while the QCD corrections show a very mild dependence on the gluino mass, apart from the region around $m_{\tilde{g}} \approx 535$ GeV. The kink that appears here, arises in the \tilde{t}_2 self-energy at the threshold where $m_{\tilde{t}_2} = m_{\tilde{g}} + m_t$.

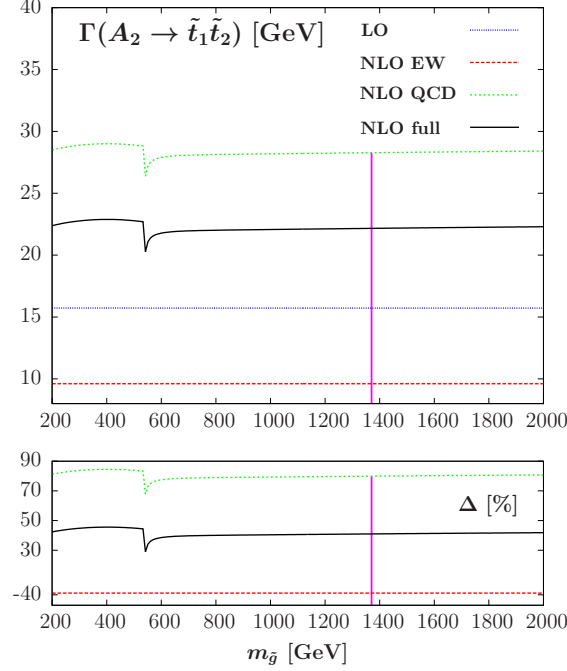


Figure 8: Upper: The partial decay width $\Gamma(A_2 \rightarrow \tilde{t}_1 \tilde{t}_2)$ as a function of $m_{\tilde{g}}$. The color and line style code is the same as in Fig. 6. Lower: The relative correction $\Delta = (\Gamma_X^{\text{NLO}} - \Gamma^{\text{LO}})/\Gamma^{\text{LO}}$ in per cent for $X = \text{QCD}$ (green/dotted), EW (red/dashed) and the full NLO corrections (black/full). The pink line shows the position of the parameter point defined in Eqs. (6.57)-(6.61).

The size of the higher order corrections sensitively depends on the scenario. Thus we find for the scenario defined by

$$\begin{aligned}
 m_{\tilde{u}_R, \tilde{c}_R} &= m_{\tilde{d}_R, \tilde{s}_R} = m_{\tilde{Q}_{1,2}} = m_{\tilde{L}_{1,2}} = m_{\tilde{e}_R, \tilde{\mu}_R} = 3 \text{ TeV}, \quad m_{\tilde{t}_R} = 714.25 \text{ GeV}, \\
 m_{\tilde{Q}_3} &= 1035 \text{ GeV}, \quad m_{\tilde{b}_R} = 2776 \text{ GeV}, \quad m_{\tilde{L}_3} = 2156 \text{ GeV}, \quad m_{\tilde{\tau}_R} = 1755 \text{ GeV}, \\
 A_t &= 1246 \text{ GeV}, \quad A_{u,c} = 1347 \text{ GeV}, \quad A_{d,s,b} = -1651 \text{ GeV}, \quad A_{e,\mu,\tau} = 769.08 \text{ GeV}, \\
 M_1 &= 460.61 \text{ GeV}, \quad M_2 = 381.55 \text{ GeV}, \quad M_3 = 2296 \text{ GeV}
 \end{aligned} \tag{6.69}$$

and

$$\begin{aligned}
 \lambda &= 0.552, \quad \kappa = 0.030, \quad A_\kappa = -173.51 \text{ GeV}, \quad \mu_{\text{eff}} = 446.80 \text{ GeV}, \\
 \tan \beta &= 3.005, \quad M_{H^\pm} = 1460 \text{ GeV},
 \end{aligned} \tag{6.70}$$

resulting in

$$M_{A_2} = 1461 \text{ GeV}, \quad m_{\tilde{t}_1} = 353.02 \text{ GeV} \quad \text{and} \quad m_{\tilde{t}_2} = 927.56 \text{ GeV} \tag{6.71}$$

and an LO decay width of

$$\Gamma^{\text{LO}}(A_2 \rightarrow \tilde{t}_1 \tilde{t}_2) = 15.24 \text{ GeV} \quad (6.72)$$

NLO QCD and EW corrections that amount to $\Delta^{\text{QCD}} = 23.4\%$ and $\Delta^{\text{EW}} = -10.2\%$, respectively, resulting in a total correction of

$$\Delta^{\text{QCD+EW}}(A_2 \rightarrow \tilde{t}_1 \tilde{t}_2) = 13.2\% . \quad (6.73)$$

This can also be inferred from Fig. 9 which shows the NLO corrections to the decay widths as a function of $m_{\tilde{t}_1}$. As demonstrated in the lower plot, the NLO QCD corrections are of the order of 20-25%, while the EW corrections range between about -17% and -8%, leading to an overall increase of the cross section between 3% and 17% due to the combined NLO corrections.

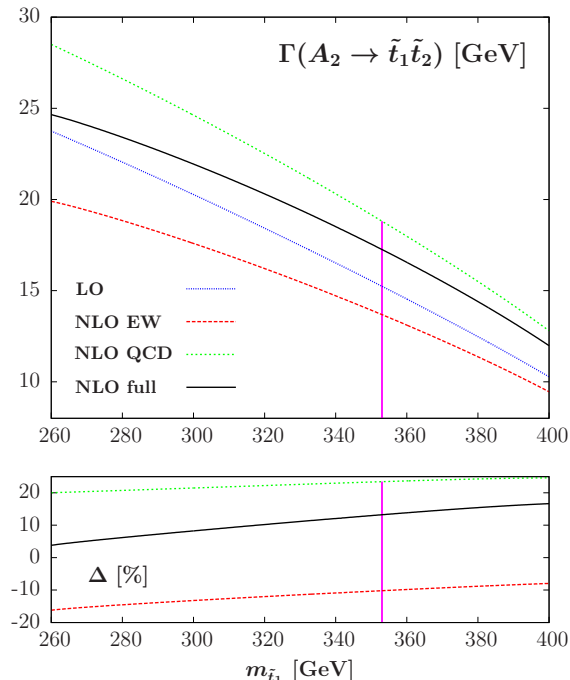


Figure 9: Same as Fig. 6, but now for the initial scenario (marked by the pink line in the plot) given by Eqs. (6.69)–(6.70)

6.2 Stop Decays into a Pseudoscalar

Decays of the heavy stop into a pseudoscalar and the light stop,

$$\tilde{t}_2 \rightarrow A_i + \tilde{t}_1 , \quad i = 1, 2 , \quad (6.74)$$

can occur and become important when there is a large mass splitting between the two stop mass eigenstates. Stop decays into a SM-like Higgs boson final state have recently been discussed in [110] and the production of NMSSM Higgs bosons in squark cascade decays in [33, 111]. The LO decay width is obtained from Eq. (3.18) by adapting the kinematic factor and dividing by

the color factor 3 and the factor 2 due to the summation of the two charge conjugated stop pair final states,

$$\Gamma^{\text{LO}}(\tilde{t}_2 \rightarrow A_i \tilde{t}_1) = \frac{\lambda^{1/2}(m_{\tilde{t}_2}^2, M_{A_i}^2, m_{\tilde{t}_1}^2)}{16\pi m_{\tilde{t}_2}^3} \left| \sum_{j=1}^2 \mathbf{Z}_{ij} G_{A_j}^{12} \right|^2. \quad (6.75)$$

The NLO SUSY-QCD decay width can be written as

$$\Gamma^{\text{NLO}}(\tilde{t}_2 \rightarrow A_i \tilde{t}_1) = \Gamma^{\text{LO}}(\tilde{t}_2 \rightarrow A_i \tilde{t}_1) + \Gamma_{\text{QCD}}^{(1)}(\tilde{t}_2 \rightarrow A_i \tilde{t}_1), \quad (6.76)$$

where

$$\Gamma_{\text{QCD}}^{(1)}(\tilde{t}_2 \rightarrow A_i \tilde{t}_1) = \text{Re} \left[\frac{\lambda^{1/2}(m_{\tilde{t}_2}^2, M_{A_i}^2, m_{\tilde{t}_1}^2)}{24\pi m_{\tilde{t}_2}^3} \left(\sum_{j=1}^2 \mathbf{Z}_{ij}^* G_{A_j}^{12*} \right) \frac{\alpha_s}{\pi} \left(\sum_{k=1}^2 \mathbf{Z}_{ik} \Delta_{k, \tilde{t}_2}^{\text{QCD}} \right) \right], \quad (6.77)$$

with the correction factor

$$\Delta_{k, \tilde{t}_2}^{\text{QCD}} = \Delta_{k, \tilde{t}_2}^V + \Delta_{k, \tilde{t}_2}^{\text{CT}} + \Delta_{k, \tilde{t}_2}^R. \quad (6.78)$$

The virtual corrections⁷ and the counterterms are given by the same expressions as for the pseudoscalar decay presented in section 4, *i.e.*

$$\Delta_{k, \tilde{t}_2}^V = \Delta_{A_k}^V \quad \text{and} \quad \Delta_{k, \tilde{t}_2}^{\text{CT}} = \Delta_{A_k}^{\text{CT}}. \quad (6.79)$$

In the real corrections, though, the roles of A_k and \tilde{t}_2 have to be interchanged,

$$\Delta_{k, \tilde{t}_2}^R = \Delta_{A_k}^R(M_{A_k}^2 \leftrightarrow m_{\tilde{t}_2}^2), \quad (6.80)$$

with $\Delta_{A_k}^R$ given in Eq. (4.41). The NLO SUSY-EW corrections are composed of the same electroweak virtual corrections to the vertex⁸, the same counterterms and the same mixing contributions of the pseudoscalar with the Z and Goldstone boson, $\Delta_{A_k}^{\text{EW}}$ and $\delta M_{\text{mix}, i}^{G, Z}$, as in the pseudoscalar decay. In the real corrections, however, again $M_{A_i}^2$ and $m_{\tilde{t}_2}^2$ have to be interchanged. We hence have

$$\Gamma_{\text{EW}}^{\text{NLO}}(\tilde{t}_2 \rightarrow A_i \tilde{t}_1) = \frac{\lambda^{1/2}}{16\pi m_{\tilde{t}_2}^3} \left[\left| \sum_{j=1}^2 \mathbf{Z}_{ij} G_{A_j}^{12} \right|^2 + \left(\sum_{j=1}^2 \mathbf{Z}_{ij}^* G_{A_j}^{12*} \right) \left(\sum_{k=1}^2 \mathbf{Z}_{ik} \Delta_{k, \tilde{t}_2}^{R, \text{EW}} \right) - 2\text{Re} \left(\sum_{j=1}^2 \mathbf{Z}_{ij}^* G_{A_j}^{12*} \left(\sum_{k=1}^2 \mathbf{Z}_{ik} \Delta_{A_k}^{\text{EW}} + \delta M_{\text{mix}, i}^{G, Z} \right) \right) \right], \quad (6.81)$$

with

$$\lambda^{1/2} \equiv \lambda^{1/2}(m_{\tilde{t}_2}^2, M_{A_i}^2, m_{\tilde{t}_1}^2) \quad (6.82)$$

⁷The diagrams are the same as in Fig. 1, but with \tilde{t}_2 in the initial and A_i in the final state.

⁸In the Feynman diagrams of Fig. 3 simply the \tilde{t}_2 leg has to be crossed to the initial and the A_i leg to the final state.

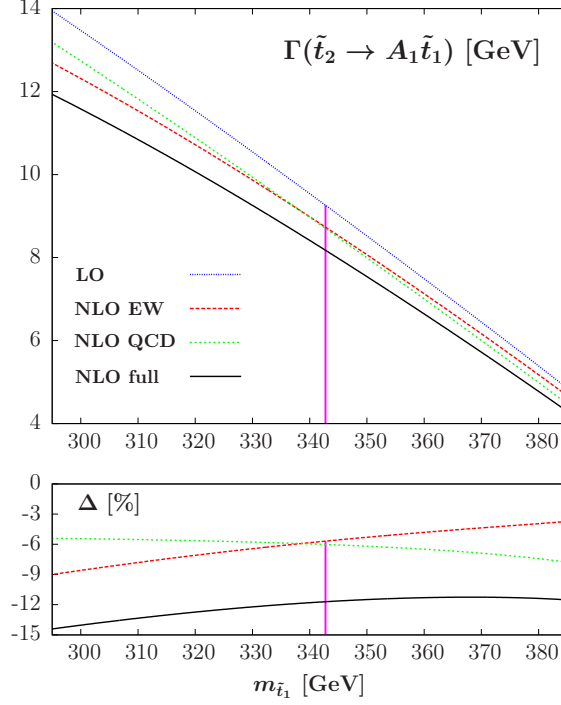


Figure 10: The decay width $\Gamma(\tilde{t}_2 \rightarrow A_1 \tilde{t}_1)$ as a function of $m_{\tilde{t}_1}$ at LO (blue/upper dotted), including the NLO QCD (green/lower dotted), the NLO EW (red/dashed) and both the EW and QCD corrections (black/full). Lower: The relative correction $\Delta = (\Gamma_X^{\text{NLO}} - \Gamma^{\text{LO}})/\Gamma^{\text{LO}}$ in per cent for $X = \text{QCD}$ (green/dotted), EW (red/dashed) and the full NLO corrections (black/full). The pink line shows the position of the parameter point defined in Eqs. (6.85)–(6.86).

and

$$\Delta_{k,\tilde{t}_2}^{R,\text{EW}} = \frac{e^2}{16\pi^2} \Delta_{A_k}^R (M_{A_k}^2 \leftrightarrow m_{\tilde{t}_2}^2) \quad (6.83)$$

and $\Delta_{A_k}^{\text{EW}}$ and $\delta M_{\text{mix},i}^{G,Z}$ given in section 5. The full NLO decay width including SUSY-QCD and -EW corrections is given by

$$\Gamma^{\text{NLO, full}} = \Gamma_{\text{EW}}^{\text{NLO}} + \Gamma_{\text{QCD}}^{(1)}, \quad (6.84)$$

with $\Gamma_{\text{QCD}}^{(1)}$ given by Eqs. (6.77)–(6.80) and $\Gamma_{\text{EW}}^{\text{NLO}}$ by Eq. (6.81).

In order to show the impact of the SUSY-EW and -QCD corrections on the stop decay width we chose the following parameter set, which leads to an NMSSM Higgs and SUSY spectrum in accordance with the LHC data:

$$\begin{aligned} m_{\tilde{u}_R, \tilde{c}_R} &= m_{\tilde{d}_R, \tilde{s}_R} = m_{\tilde{Q}_{1,2}} = m_{\tilde{L}_{1,2}} = m_{\tilde{e}_R, \tilde{\mu}_R} = 3 \text{ TeV}, \quad m_{\tilde{t}_R} = 748.07 \text{ GeV}, \\ m_{\tilde{Q}_3} &= 1259 \text{ GeV}, \quad m_{\tilde{b}_R} = 1709 \text{ GeV}, \quad m_{\tilde{L}_3} = 1637 \text{ GeV}, \quad m_{\tilde{\tau}_R} = 1618 \text{ GeV}, \\ A_t &= 1589 \text{ GeV}, \quad A_{u,c} = 1675 \text{ GeV}, \quad A_{d,s,b} = -669.04 \text{ GeV}, \quad A_{e,\mu,\tau} = 179.93 \text{ GeV}, \\ M_1 &= 645.51 \text{ GeV}, \quad M_2 = 272.11 \text{ GeV}, \quad M_3 = 2511 \text{ GeV}, \end{aligned} \quad (6.85)$$

and the NMSSM specific input parameters

$$\begin{aligned} \lambda &= 0.588, \quad \kappa = 0.378, \quad A_\kappa = -675.73 \text{ GeV}, \quad \mu_{\text{eff}} = 385.90 \text{ GeV}, \\ \tan \beta &= 1.529, \quad M_{H^\pm} = 639.08 \text{ GeV}. \end{aligned} \quad (6.86)$$

This results in the two-loop corrected mass M_{A_1} of the lighter pseudoscalar A_1 and the stop masses $m_{\tilde{t}_{1,2}}$,

$$M_{A_1} = 637.40 \text{ GeV} , \quad m_{\tilde{t}_1} = 342.76 \text{ GeV} \quad \text{and} \quad m_{\tilde{t}_2} = 1153 \text{ GeV} . \quad (6.87)$$

And for the stop soft SUSY breaking trilinear coupling in the OS scheme we get

$$A_t^{\text{OS}} = 1675 \text{ GeV} . \quad (6.88)$$

Figure 10 (upper) shows the decay width $\Gamma(\tilde{t}_2 \rightarrow A_1 \tilde{t}_1)$ at LO, including the NLO EW, the NLO QCD and both NLO corrections, as a function of $m_{\tilde{t}_1}$, varied around the chosen parameter point, marked by the pink line in the plots. The LO decay width reaches

$$\Gamma^{\text{LO}}(\tilde{t}_2 \rightarrow A_1 \tilde{t}_1) = 9.26 \text{ GeV} . \quad (6.89)$$

In the whole investigated $m_{\tilde{t}_1}$ range, the EW and QCD corrections are significant, decreasing together the LO width by $\sim 12 - 15\%$. Both corrections are of similar size, where, depending on the parameter point, once the QCD, once the EW corrections are more important. At our starting parameter point both corrections are almost equal resulting in a decrease of

$$\Delta\Gamma^{\text{QCD+EW}} = -11.7\% , \quad (6.90)$$

cf. Fig. 10 (lower). Our results demonstrate that also in the stop decays both the QCD and EW corrections have to be considered for a meaningful prediction of the stop decay width.

7 Conclusions

The search for New Physics is one of the main tasks at the LHC. In the absence of any direct sign of new resonances so far, the precise investigation of the Higgs sector becomes more and more important. Physics beyond the SM might reveal itself in modified Higgs decay rates compared to the SM expectations or in the discovery of additional Higgs bosons, unambiguous sign of a non-SM Higgs sector. In view of the complexity of the experimental analyses and the plethora of still possible New Physics extensions, it is evident that the success of this research program depends on the precise predictions of parameters and observables from the theory side. In this paper we have calculated the NLO SUSY-EW and -QCD corrections to the decays of a pseudoscalar NMSSM Higgs boson into stop pairs and of the heavier stop into the lighter stop and a pseudoscalar Higgs boson. Both processes can become important in certain regions of the parameter space and hence contribute to the discovery channels of either the pseudoscalar Higgs boson and/or the stop quarks. The NLO corrections turn out to be important and, depending on the scenario, the EW corrections can be of same size as the QCD corrections and also come with opposite sign. Therefore not only the inclusion of higher order corrections is important but also the consideration of both the QCD and the EW corrections is indispensable for making reliable predictions.

Acknowledgments

JB, MM and KW have been supported in part by the DFG SFB/TR9 “Computational Particle Physics” and furthermore JB in part by the Institutional Strategy of the University of Tübingen (DFG, ZUK 63). The authors thank Michael Spira for helpful discussions.

Appendix

A The Loop Functions

The D dimensional one-loop integrals encountered in the calculation are the scalar one-, two- and three-point functions A_0 , B_0 and C_0 as well as the coefficient of the two-point tensor integral of rank one, B_1 . They are defined as

$$A_0(m) = 16\pi^2\mu^{4-D} \int \frac{d^D q}{i(2\pi)^D} \frac{1}{(q^2 - m^2)} \quad (\text{A.1})$$

$$B_0(p^2; m_1, m_2) = 16\pi^2\mu^{4-D} \int \frac{d^D q}{i(2\pi)^D} \frac{1}{(q^2 - m_1^2)[(q+p)^2 - m_2^2]} \quad (\text{A.2})$$

$$C_0(p_1^2, p_2^2, p_{12}^2; m_1, m_2, m_3) = 16\pi^2\mu^{4-D} \int \frac{d^D q}{i(2\pi)^D} \times \frac{1}{(q^2 - m_1^2)[(q+p_1)^2 - m_2^2][(q+p_{12})^2 - m_3^2]} \quad (\text{A.3})$$

$$p_\mu B_1(p^2; m_1, m_2) = 16\pi^2\mu^{4-D} \int \frac{d^D q}{i(2\pi)^D} \frac{q_\mu}{(q^2 - m_1^2)[(q+p)^2 - m_2^2]}, \quad (\text{A.4})$$

where

$$p_{12} \equiv p_1 + p_2 \quad (\text{A.5})$$

with p, p_1, p_2 denoting the external momenta, which are taken as incoming, and m, m_1, m_2, m_3 the masses of the loop particles.

References

- [1] G. Aad *et al.* [ATLAS Collaboration], Phys. Lett. B **716** (2012) 1 [arXiv:1207.7214 [hep-ex]]; G. Aad *et al.* [ATLAS Collaboration], ATLAS-CONF-2012-162.
- [2] S. Chatrchyan *et al.* [CMS Collaboration], Phys. Lett. B **716** (2012) 30 [arXiv:1207.7235 [hep-ex]]; S. Chatrchyan *et al.* [CMS Collaboration], CMS-PAS-HIG-12-045.
- [3] D.V. Volkov and V.P. Alkulov, Phys. Lett. **B46** (1973) 109; J. Wess and B. Zumino, Nucl. Phys. **B70** (1974) 39; P. Fayet, Phys. Lett. **B64** (1976) 159, Phys. Lett. **B69** (1977) 489, Phys. Lett. **B84** (1979) 416; G.F. Farrar and P. Fayet, Phys. Lett. **B76** (1978) 575; S. Dimopoulos and H. Georgi, Nucl. Phys. **B193** (1981) 150; N. Sakai, Z. Phys. **C11** (1981) 153; E. Witten, Nucl. Phys. **B188** (1981) 513; H.P. Nilles, Phys. Rep. **110** (1984) 1; H.E. Haber and G.L. Kane, Phys. Rep. **117** (1985) 75; M.F. Sohnius, Phys. Rep. **128** (1985) 39; J.F. Gunion and H.E. Haber, Nucl. Phys. **B272** (1986) 1 [Erratum-ibid. **B402** (1993) 567], Nucl. Phys. **B278** (1986) 449; A.B. Lahanas and D.V. Nanopoulos, Phys. Rep. **145** (1987) 1.
- [4] P. Fayet, Nucl. Phys. **B90** (1975) 104; R. Barbieri, S. Ferrara, C. A. Savoy, Phys. Lett. **B119** (1982) 343; M. Dine, W. Fischler, M. Srednicki, Phys. Lett. **B104** (1981) 199; H. P. Nilles, M. Srednicki, D. Wyler, Phys. Lett. **B120** (1983) 346; J. M. Frere,

- D. R. T. Jones, S. Raby, Nucl. Phys. **B222** (1983) 11; J. P. Derendinger, C. A. Savoy, Nucl. Phys. **B237** (1984) 307; J. R. Ellis, J. F. Gunion, H. E. Haber, L. Roszkowski, F. Zwirner, Phys. Rev. **D39** (1989) 844; M. Drees, Int. J. Mod. Phys. **A4** (1989) 3635; U. Ellwanger, M. Rausch de Traubenberg, C. A. Savoy, Phys. Lett. **B315** (1993) 331 [hep-ph/9307322], Z. Phys. **C67** (1995) 665 [hep-ph/9502206], Nucl. Phys. **B492** (1997) 21 [hep-ph/9611251]; T. Elliott, S. F. King, P. L. White, Phys. Lett. **B351** (1995) 213 [hep-ph/9406303]; S. F. King, P. L. White, Phys. Rev. **D52** (1995) 4183 [hep-ph/9505326]; F. Franke, H. Fraas, Int. J. Mod. Phys. **A12** (1997) 479 [hep-ph/9512366]; M. Maniatis, Int. J. Mod. Phys. **A25** (2010) 3505 [arXiv:0906.0777 [hep-ph]]; U. Ellwanger, C. Hugonie, A. M. Teixeira, Phys. Rept. **496** (2010) 1 [arXiv:0910.1785 [hep-ph]].
- [5] J.E. Kim and H.P. Nilles, Phys. Lett. **B138** (1984) 150.
- [6] M. Bastero-Gil, C. Hugonie, S. F. King, D. P. Roy and S. Vempati, Phys. Lett. B **489**, 359 (2000) [hep-ph/0006198]; A. Delgado, C. Kolda, J. P. Olson and A. de la Puente, Phys. Rev. Lett. **105**, 091802 (2010) [arXiv:1005.1282 [hep-ph]]; U. Ellwanger, G. Espitalier-Noel and C. Hugonie, JHEP **1109** (2011) 105 [arXiv:1107.2472 [hep-ph]]; G. G. Ross and K. Schmidt-Hoberg, arXiv:1108.1284 [hep-ph]; L. J. Hall, D. Pinner and J. T. Ruderman, JHEP **1204** (2012) 131 [arXiv:1112.2703 [hep-ph]]; Z. Kang, J. Li and T. Li, JHEP **1211** (2012) 024 [arXiv:1201.5305 [hep-ph]]; J. -J. Cao, Z. -X. Heng, J. M. Yang, Y. -M. Zhang and J. -Y. Zhu, JHEP **1203** (2012) 086 [arXiv:1202.5821 [hep-ph]]; J. Cao, Z. Heng, J. M. Yang and J. Zhu, JHEP **1210** (2012) 079 [arXiv:1207.3698 [hep-ph]]; J. R. Espinosa, C. Grojean, V. Sanz and M. Trott, JHEP **1212** (2012) 077 [arXiv:1207.7355 [hep-ph]]; M. Perelstein and B. Shakya, Phys. Rev. D **88** (2013) 075003 [arXiv:1208.0833 [hep-ph]]; K. Agashe, Y. Cui and R. Franceschini, JHEP **1302** (2013) 031 [arXiv:1209.2115 [hep-ph]].
- [7] S. F. King, M. Mühlleitner and R. Nevzorov, Nucl. Phys. B **860** (2012) 207 [arXiv:1201.2671 [hep-ph]]; S. F. King, M. Mühlleitner, R. Nevzorov and K. Walz, Nucl. Phys. B **870** (2013) 323 [arXiv:1211.5074 [hep-ph]].
- [8] S. F. King, M. Mühlleitner, R. Nevzorov and K. Walz, Phys. Rev. D **90** (2014) 9, 095014 [arXiv:1408.1120 [hep-ph]].
- [9] U. Ellwanger, Phys. Lett. B **698** (2011) 293 [arXiv:1012.1201 [hep-ph]]; U. Ellwanger, JHEP **1203** (2012) 044 [arXiv:1112.3548 [hep-ph]]; A. Arvanitaki and G. Villadoro, JHEP **1202** (2012) 144 [arXiv:1112.4835 [hep-ph]].
- [10] J. F. Gunion, Y. Jiang and S. Kraml, Phys. Rev. D **86** (2012) 071702 [arXiv:1207.1545 [hep-ph]].
- [11] J. F. Gunion, Y. Jiang and S. Kraml, Phys. Rev. Lett. **110** (2013) 051801 [arXiv:1208.1817 [hep-ph]].
- [12] Z. Kang, J. Li, T. Li, D. Liu and J. Shu, Phys. Rev. D **88** (2013) 1, 015006 [arXiv:1301.0453 [hep-ph]].
- [13] D. G. Cerdeno, P. Ghosh and C. B. Park, JHEP **1306** (2013) 031 [arXiv:1301.1325 [hep-ph]].
- [14] M. Badziak, M. Olechowski and S. Pokorski, JHEP **1306** (2013) 043 [arXiv:1304.5437 [hep-ph]].

- [15] S. Munir, L. Roszkowski and S. Trojanowski, Phys. Rev. D **88** (2013) 5, 055017 [arXiv:1305.0591 [hep-ph]].
- [16] D. T. Nhung, M. Mühlleitner, J. Streicher and K. Walz, JHEP **1311** (2013) 181 [arXiv:1306.3926 [hep-ph]].
- [17] U. Ellwanger, JHEP **1308** (2013) 077 [arXiv:1306.5541 [hep-ph]].
- [18] D. G. Cerdeno, P. Ghosh, C. B. Park and M. Peiro, JHEP **1402** (2014) 048 [arXiv:1307.7601 [hep-ph]].
- [19] C. Beskidt, W. de Boer and D. I. Kazakov, Phys. Lett. B **726** (2013) 758 [arXiv:1308.1333 [hep-ph]].
- [20] K. Choi, S. H. Im, K. S. Jeong and M. -S. Seo, JHEP **1401** (2014) 072 [arXiv:1308.4447 [hep-ph]].
- [21] J. Kozaczuk and S. Profumo, Phys. Rev. D **89** (2014) 095012 [arXiv:1308.5705 [hep-ph]].
- [22] J. Cao, F. Ding, C. Han, J. M. Yang and J. Zhu, JHEP **1311** (2013) 018 [arXiv:1309.4939 [hep-ph]].
- [23] J.-W. Fan, J.-Q. Tao, Y.-Q. Shen, G.-M. Chen, H.-S. Chen, S. Gascon-Shotkin, M. Lethuillier and L. Sgandurra *et al.*, Chin. Phys. C **38** (2014) 073101 [arXiv:1309.6394 [hep-ph]].
- [24] J. Huang, T. Liu, L. -T. Wang and F. Yu, Phys. Rev. Lett. **112** (2014) 221803 [arXiv:1309.6633 [hep-ph]].
- [25] S. Munir, Phys. Rev. D **89** (2014) 095013 [arXiv:1310.8129 [hep-ph]].
- [26] G. Belanger, V. Bizouard and G. Chalons, Phys. Rev. D **89** (2014) 095023 [arXiv:1402.3522 [hep-ph]].
- [27] C. Beskidt, W. de Boer and D. I. Kazakov, Phys. Lett. B **738** (2014) 505 [arXiv:1402.4650 [hep-ph]].
- [28] U. Ellwanger and C. Hugonie, JHEP **1408** (2014) 046 [arXiv:1405.6647 [hep-ph]].
- [29] U. Ellwanger and A. M. Teixeira, JHEP **1410** (2014) 113 [arXiv:1406.7221 [hep-ph]].
- [30] D. Das, L. Mitzka and W. Porod, arXiv:1408.1704 [hep-ph].
- [31] J. Cao, D. Li, L. Shang, P. Wu and Y. Zhang, JHEP **1412** (2014) 026 [arXiv:1409.8431 [hep-ph]].
- [32] N. E. Bomark, S. Moretti, S. Munir and L. Roszkowski, JHEP **1502** (2015) 044 [arXiv:1409.8393 [hep-ph]].
- [33] U. Ellwanger and A. M. Teixeira, JHEP **1504** (2015) 172 [arXiv:1412.6394 [hep-ph]].
- [34] S. Moretti and S. Munir, arXiv:1505.00545 [hep-ph].
- [35] D. Buttazzo, F. Sala and A. Tesi, arXiv:1505.05488 [hep-ph].
- [36] C. T. Potter, arXiv:1505.05554 [hep-ph].

- [37] A. Djouadi, J. Kalinowski, P. Ohmann and P. M. Zerwas, Z. Phys. C **74** (1997) 93 [hep-ph/9605339].
- [38] A. Djouadi, P. Janot, J. Kalinowski and P. M. Zerwas, Phys. Lett. B **376** (1996) 220 [hep-ph/9603368].
- [39] A. Bartl, H. Eberl, K. Hidaka, T. Kon, W. Majerotto and Y. Yamada, Phys. Lett. B **402** (1997) 303 [hep-ph/9701398].
- [40] A. Arhrib, A. Djouadi, W. Hollik and C. Junger, Phys. Rev. D **57** (1998) 5860 [hep-ph/9702426].
- [41] H. Eberl, K. Hidaka, S. Kraml, W. Majerotto and Y. Yamada, Phys. Rev. D **62** (2000) 055006 [hep-ph/9912463].
- [42] E. Accomando, G. Chachamis, F. Fugel, M. Spira and M. Walser, Phys. Rev. D **85** (2012) 015004 [arXiv:1103.4283 [hep-ph]].
- [43] C. Weber, H. Eberl and W. Majerotto, Phys. Lett. B **572** (2003) 56 [hep-ph/0305250]; Phys. Rev. D **68**, 093011 (2003) [hep-ph/0308146]. .
- [44] A. Bartl, H. Eberl, K. Hidaka, S. Kraml, T. Kon, W. Majerotto, W. Porod and Y. Yamada, Phys. Lett. B **435** (1998) 118 [hep-ph/9804265].
- [45] A. Bartl, H. Eberl, K. Hidaka, S. Kraml, W. Majerotto, W. Porod and Y. Yamada, Phys. Rev. D **59** (1999) 115007 [hep-ph/9806299].
- [46] S. Heinemeyer, H. Rzehak and C. Schappacher, Phys. Rev. D **82** (2010) 075010 [arXiv:1007.0689 [hep-ph]].
- [47] M. Krämer and M. Mühlleitner, arXiv:1501.06658 [hep-ph].
- [48] U. Ellwanger, Phys.Lett. **B303**, 271 (1993) [hep-ph/9302224].
- [49] T. Elliott, S. King, and P. White, Phys.Lett. **B305**, 71 (1993) [hep-ph/9302202].
- [50] T. Elliott, S. King, and P. White, Phys.Lett. **B314**, 56 (1993) [hep-ph/9305282].
- [51] T. Elliott, S. King, and P. White, Phys.Rev. **D49**, 2435 (1994) [hep-ph/9308309].
- [52] P. Pandita, Z.Phys. **C59**, 575 (1993).
- [53] U. Ellwanger and C. Hugonie, Phys.Lett. **B623**, 93 (2005) [hep-ph/0504269].
- [54] G. Degrandi and P. Slavich, Nucl. Phys. B **825** (2010) 119 [arXiv:0907.4682 [hep-ph]].
- [55] F. Staub, W. Porod, and B. Herrmann, JHEP **1010**, 040 (2010) [arXiv:1007.4049 [hep-ph]].
- [56] K. Ender, T. Graf, M. Mühlleitner and H. Rzehak, Phys. Rev. D **85** (2012) 075024 [arXiv:1111.4952 [hep-ph]].
- [57] M. D. Goodsell, K. Nickel and F. Staub, Phys. Rev. D **91** (2015) 3, 035021 [arXiv:1411.4665 [hep-ph]].
- [58] M. Goodsell, K. Nickel and F. Staub, arXiv:1503.03098 [hep-ph].

- [59] U. Ellwanger, J. F. Gunion, and C. Hugonie, JHEP **0502**, 066 (2005) [hep-ph/0406215].
- [60] U. Ellwanger and C. Hugonie, Comput. Phys. Commun. **175**, 290 (2006) [hep-ph/0508022].
- [61] U. Ellwanger and C. Hugonie, Comput. Phys. Commun. **177**, 399 (2007) [hep-ph/0612134].
- [62] B. Allanach, Comput. Phys. Commun. **143**, 305 (2002) [hep-ph/0104145].
- [63] B. Allanach, P. Athron, L. C. Tunstall, A. Voigt, and A. Williams, Comput. Phys. Commun. **185**, 2322 (2014) [arXiv:1311.7659 [hep-ph]].
- [64] F. Staub, Comput. Phys. Commun. **182**, 808 (2011) [arXiv:1002.0840 [hep-ph]].
- [65] F. Staub, Comput. Phys. Commun. **184**, 1792 (2013) [arXiv:1207.0906 [hep-ph]].
- [66] F. Staub, Comput. Phys. Commun. **185**, 1773 (2014) [arXiv:1309.7223 [hep-ph]].
- [67] M. D. Goodsell, K. Nickel and F. Staub, Eur. Phys. J. C **75** (2015) 1, 32 [arXiv:1411.0675 [hep-ph]].
- [68] W. Porod, Comput. Phys. Commun. **153**, 275 (2003) [hep-ph/0301101].
- [69] W. Porod and F. Staub, Comput. Phys. Commun. **183**, 2458 (2012) [arXiv:1104.1573 [hep-ph]].
- [70] P. Athron, J. h. Park, D. Stöckinger and A. Voigt, Comput. Phys. Commun. **190**, 139 (2015) [arXiv:1406.2319 [hep-ph]].
- [71] P. Athron, J. h. Park, D. Stöckinger and A. Voigt, arXiv:1410.7385 [hep-ph].
- [72] F. Domingo, arXiv:1503.07087 [hep-ph].
- [73] J. Baglio, R. Gröber, M. Mühlleitner, D. T. Nhung, H. Rzehak, M. Spira, J. Streicher and K. Walz, Comput. Phys. Commun. **185** (2014) 12, 3372 [arXiv:1312.4788 [hep-ph]].
- [74] T. Graf, R. Gröber, M. Mühlleitner, H. Rzehak and K. Walz, JHEP **1210** (2012) 122 [arXiv:1206.6806 [hep-ph]].
- [75] M. Mühlleitner, D. T. Nhung, H. Rzehak and K. Walz, arXiv:1412.0918 [hep-ph].
- [76] S. Liebler, Eur. Phys. J. C **75** (2015) 5, 210 [arXiv:1502.07972 [hep-ph]].
- [77] M. Frank, T. Hahn, S. Heinemeyer, W. Hollik, H. Rzehak and G. Weiglein, JHEP **0702** (2007) 047 [hep-ph/0611326].
- [78] W. Siegel, Phys. Lett. B **84** (1979) 193; D. M. Capper, D. R. T. Jones and P. van Nieuwenhuizen, Nucl. Phys. B **167** (1980) 479.
- [79] G. 't Hooft and M.J.G. Veltman, Nucl. Phys. B **153** (1979) 365; G. Passarino and M.J.G. Veltman, Nucl. Phys. B **160** (1979) 151.
- [80] T. Hahn, Comput. Phys. Commun. **140** (2001) 418 [hep-ph/0012260]; T. Hahn and C. Schappacher, Comput. Phys. Commun. **143** (2002) 54 [hep-ph/0105349].

- [81] T. Hahn and M. Perez-Victoria, Comput. Phys. Commun. **118** (1999) 153 [hep-ph/9807565]; T. Hahn, Comput. Phys. Commun. **178** (2008) 217 [hep-ph/0611273].
- [82] A. Djouadi, M. Spira and P.M. Zerwas, Phys. Lett. B **264** (1991) 440 and Z. Phys. C **70** (1996) 427; M. Spira *et al.*, Nucl. Phys. B **453** (1995) 17; A. Djouadi, J. Kalinowski and M. Spira, Comput. Phys. Commun. **108** (1998) 56; J. M. Butterworth, A. Arbey, L. Basso, S. Belov, A. Bharucha, F. Braam, A. Buckley and M. Campanelli *et al.*, arXiv:1003.1643 [hep-ph].
- [83] A. Djouadi, M. M. Mühlleitner and M. Spira, Acta Phys. Polon. **B38** (2007) 635 [hep-ph/0609292].
- [84] M. Mühlleitner, A. Djouadi and Y. Mambrini, Comput. Phys. Commun. **168** (2005) 46 [hep-ph/0311167]; M. Mühlleitner, Acta Phys. Polon. **B35** (2004) 2753 [hep-ph/0409200].
- [85] A. Dabelstein, Z. Phys. C **67** (1995) 495 [hep-ph/9409375]; A. Dabelstein, Nucl. Phys. B **456** (1995) 25 [hep-ph/9503443].
- [86] P. Bechtle, O. Brein, S. Heinemeyer, G. Weiglein and K. E. Williams, Comput. Phys. Commun. **181** (2010) 138 [arXiv:0811.4169 [hep-ph]]; P. Bechtle, O. Brein, S. Heinemeyer, G. Weiglein and K. E. Williams, Comput. Phys. Commun. **182** (2011) 2605 [arXiv:1102.1898 [hep-ph]]; P. Bechtle, O. Brein, S. Heinemeyer, O. Stal, T. Stefaniak, G. Weiglein and K. E. Williams, Eur. Phys. J. C **74** (2014) 2693 [arXiv:1311.0055 [hep-ph]].
- [87] P. Bechtle, S. Heinemeyer, O. Stal, T. Stefaniak and G. Weiglein, Eur. Phys. J. C **74** (2014) 2711 [arXiv:1305.1933 [hep-ph]].
- [88] T. Inami, T. Kubota, and Y. Okada, Z.Phys. **C18**, 69 (1983).
- [89] A. Djouadi, M. Spira, and P. Zerwas, Phys.Lett. **B264**, 440 (1991).
- [90] M. Spira, A. Djouadi, D. Graudenz, and P. Zerwas, Phys.Lett. **B318**, 347 (1993).
- [91] M. Spira, A. Djouadi, D. Graudenz, and P. Zerwas, Nucl.Phys. **B453**, 17 (1995), hep-ph/9504378.
- [92] M. Krämer, E. Laenen, and M. Spira, Nucl.Phys. **B511**, 523 (1998), hep-ph/9611272.
- [93] K. Chetyrkin, B. A. Kniehl, and M. Steinhauser, Phys.Rev.Lett. **79**, 353 (1997), hep-ph/9705240.
- [94] K. Chetyrkin, B. A. Kniehl, and M. Steinhauser, Nucl.Phys. **B510**, 61 (1998), hep-ph/9708255.
- [95] Y. Schröder and M. Steinhauser, JHEP **0601**, 051 (2006), hep-ph/0512058.
- [96] K. Chetyrkin, J. H. Kühn, and C. Sturm, Nucl.Phys. **B744**, 121 (2006), hep-ph/0512060.
- [97] P. Baikov and K. Chetyrkin, Phys.Rev.Lett. **97**, 061803 (2006), hep-ph/0604194.
- [98] S. Dawson, A. Djouadi, and M. Spira, Phys.Rev.Lett. **77**, 16 (1996), hep-ph/9603423.

- [99] A. Djouadi, V. Driesen, W. Hollik, and J. I. Illana, Eur.Phys.J. **C1**, 149 (1998), hep-ph/9612362.
- [100] G. Aad *et al.* [ATLAS Collaboration], Phys. Rev. Lett. **109** (2012) 211802 [arXiv:1208.1447 [hep-ex]]; Phys. Rev. Lett. **109** (2012) 211803 [arXiv:1208.2590 [hep-ex]]; JHEP **1211** (2012) 094 [arXiv:1209.4186 [hep-ex]]; JHEP **1406** (2014) 124 [arXiv:1403.4853 [hep-ex]]; JHEP **1409** (2014) 015 [arXiv:1406.1122 [hep-ex]] and arXiv:1412.4742 [hep-ex].
- [101] G. Aad *et al.* [ATLAS Collaboration], JHEP **1411** (2014) 118 [arXiv:1407.0583 [hep-ex]].
- [102] G. Aad *et al.* [ATLAS Collaboration], Phys. Rev. D **90** (2014) 5, 052008 [arXiv:1407.0608 [hep-ex]].
- [103] S. Chatrchyan *et al.* [CMS Collaboration], Eur. Phys. J. C **73** (2013) 12, 2677 [arXiv:1308.1586 [hep-ex]]; S. Chatrchyan *et al.* [CMS Collaboration], Phys. Rev. Lett. **112** (2014) 161802 [arXiv:1312.3310 [hep-ex]]; V. Khachatryan *et al.* [CMS Collaboration], Phys. Rev. D **91** (2015) 052018 [arXiv:1502.00300 [hep-ex]]; CMS Collaboration, CMS-PAS-SUS-13-015, -024 and CMS-PAS-SUS-14-011.
- [104] The CMS Collaboration, CMS-PAS-SUS-13-009.
- [105] K. A. Olive *et al.* [Particle Data Group Collaboration], Chin. Phys. C **38** (2014) 090001.
- [106] F. Jegerlehner, Nuovo Cim. C **034S1** (2011) 31 [arXiv:1107.4683 [hep-ph]].
- [107] P. Z. Skands *et al.*, JHEP **0407** (2004) 036 [hep-ph/0311123]; B. C. Allanach *et al.*, Comput. Phys. Commun. **180** (2009) 8 [arXiv:0801.0045 [hep-ph]].
- [108] M. Mühlleitner and E. Popena, JHEP **1104** (2011) 095 [arXiv:1102.5712 [hep-ph]].
- [109] R. Gröber, M. Mühlleitner, E. Popena and A. Wlotzka, arXiv:1408.4662 [hep-ph].
- [110] D. Ghosh, Phys. Rev. D **88** (2013) 11, 115013 [arXiv:1308.0320 [hep-ph]].
- [111] A. Chakraborty, D. K. Ghosh, S. Mondal, S. Poddar and D. Sengupta, arXiv:1503.07592 [hep-ph].